55p

NASA SP-19

55
60p
N63-11509
Code 1

SESSION M

~~Propellants~~ ~~Chemical~~ Rocket Propulsion

Chairman, WALTER T. OLSON

DR. WALTER T. OLSON *is Chief of the Chemistry and Energy Conversion Division of the NASA Lewis Research Center. Appointed to the Lewis staff in 1942, he has conducted, supervised and reported research on fuels and combustion programs for turbojet, ramjet, and rocket engines. Dr. Olson has also served as a consultant to the Department of Defense and the U.S. Air Force. He was graduated from DePauw University in 1939 with a B.S. degree in Chemistry, earning his M.S. and Ph. D. degrees in Chemistry and Chemical Engineering from Case Institute of Technology in 1940 and 1942, respectively. Dr. Olson is an Associate Fellow of the Institute of the Aerospace Sciences, a Director of the Combustion Institute and a member of the American Chemical Society and the American Rocket Society.*

Introduction

By WALTER T. OLSON

The status of some of the key technology of the chemical rocket system is reviewed in this Session. In this review it is hoped that (1) the current problems in this technology will be revealed, (2) the fundamental physical principles involved in these problems will be made apparent, and (3) the directions in which solutions probably will lie will be indicated.

A sonde, satellite, space probe, or manned spacecraft requires for its mission a specified amount of kinetic energy, more often expressed as a velocity. With regard to rocket-propulsion, the speed imparted to the payload depends on just two items: the energy per pound of propellant and the amount of propellant that is carried. The former is specific impulse, is expressed as seconds, and is dependent on propellant chemistry; the latter is mass ratio and is dependent on vehicle design. Figure 1 shows the relations. For example, an RP–1 (kerosene)—liquid-oxygen engine in a vehicle in which 92 percent of the initial weight is consumable could provide a velocity to the payload of 27,000 feet per second (92 percent is a number that is commensurate with several large vehicles using this propellant). If the thrusting is done near the earth, 32.2 feet per second must be deducted for each second of burning. About 10,000 feet per second must be deducted for a 5-minute launch because of work against gravity; therefore, 17,000 feet per second is the net velocity for this example. Other corrections can be ignored for the present purposes.

Of course, one rocket vehicle can be made the payload on another, larger vehicle—by staging—to build up the ultimate flight velocity needed.

The inherent simplicity and instant readiness of solid propellants makes them useful for many applications: launching of smaller satellite payloads, as in Scout; orbital changes or injection, as in Echo, Tiros, or Surveyor; stage separation and emergency escape, as in Mercury, Gemini, and Apollo. Their great value in the military mission need not be detailed.

Over the years since the first asphalt—potassium perchlorate and double-base powders, the specific-impulse performance of solids has risen from about 180 pounds per pound per second to values for today's composite propellants of about 245 seconds (on a 1000-lb/sq in. chamber pressure basis). Further gains, however, are difficult. Expenditures of many millions of dollars in the last half dozen years in an attempt to find new ingredients for higher specific impulse have made specific-impulse values of the order of 300 seconds appear possible, but probably at the expense of the physical properties of the grain. Best gains in the performance of solid rockets have come from improving the mass ratio. Innovations such as high-tensile steels, cases wound from high-tensile glass filaments, and composite structures for nozzles have boosted propellant loadings to as much as 0.87 to 0.91 of the vehicle gross weight.

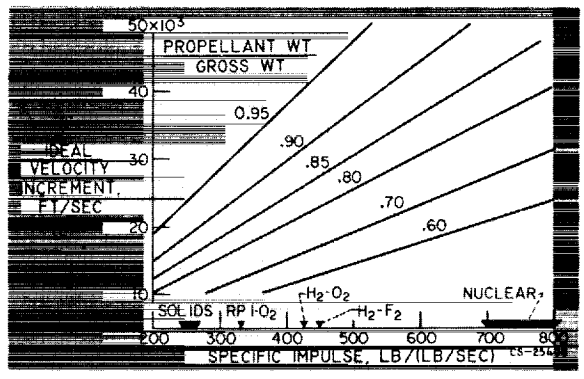

FIGURE 1.—Rocket vehicle performance.

Not shown on figure 1, but performing in the range between solids and RP–1—liquid oxygen, are propellants like nitric acid and alkyl-hydrazine mixtures. Having the advantage of being liquids at room temperatures, they are useful in space rockets like Agena, the Mariner course-correction engine, and the lunar excursion module of Apollo.

The higher end of performance including even reasonably stable chemicals, is represented by hydrogen-oxygen and hydrogen-flourine. Addition of metals like beryllium or lithium to these systems improves the specific impulse, but this approach requires a very high weight fraction of hydrogen, which makes a poor density for the system, and also adds the complexity of feeding and burning metal.

For reference, the coming first generation of nuclear heat-transfer rockets is shown, with performance at 700 seconds for hydrogen at 2672° F to 800 seconds at 3500° F. With a propellant density about one-fifth to one-twentieth that of chemical rockets, with an inherently heavier powerplant, and with the necessity of shielding, nuclear heat-transfer rockets as presently conceived have a long, rough, and expensive road before they will be able to compete in performance with chemical rockets. Propellant fractions will certainly have to exceed 0.75 of gross weight. Therefore, chemical rocket systems will be used for a long time, and it is vital to the space program that they be made as efficient and reliable as possible.

The particular propellants to which the discussion of this Session are directed are RP–1—liquid oxygen and hydrogen-oxygen, although much of what is presented is broadly applicable to more than these propellants alone. Time does not permit detailed discussion of other liquids or of solids. Furthermore, these propellants are prominent in the several principal engine programs of NASA as seen in figure 2. These engines are vital to many of our foreseeable space flights, particularly manned flights.

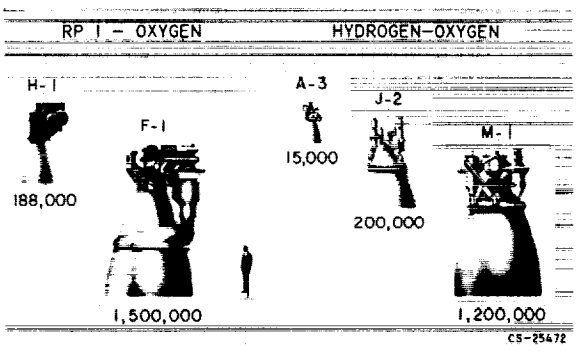

FIGURE 2.—NASA chemical rocket engines and pounds of thrust produced.

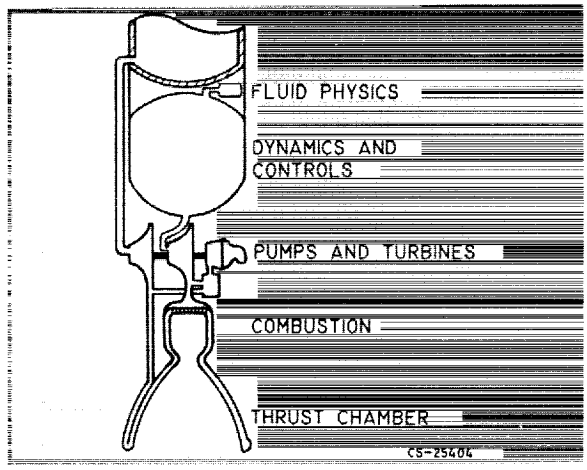

FIGURE 3.—Chemical rocket.

The H–1 engine is an outgrowth of the Thor and Atlas engines; a cluster of eight of these engines drives the Saturn C–1 booster. The F–1 engine is currently in development and will power launch vehicles for manned lunar flight. The three hydrogen-oxygen engines are for various upper stages of lunar vehicles. They signify a heavy reliance of the NASA space program on hydrogen-oxygen. Consequently, a large technology effort is progressing on this combination, which should have its first successful flight in the Centaur vehicle, powered by two of the A–3 chambers. The J–2 engine, in development, is for upper stages of Saturn for manned lunar flight. The M–1 engine is for still larger launch vehicles.

Figure 3 shows the five topics of the chemical rocket discussed in this Session: fluid systems, pumps and turbines, combustion, thrust chambers, and dynamics and controls. The physical principles, the understanding and mastery of which are vital to successful engineering of rocket-propulsion systems, are discussed.

BIBLIOGRAPHY

GRELACHI, C. J. and TANNENBAUM, S.: Survey of Current Storable Propellant. ARS Jour., vol. 32, no. 8, Aug. 1962, pp. 1189–1195.

OLSON, WALTER T.: Problems of High Energy Propellants for Rockets. Rocket and Missile Technology, Chem. Eng. Prog. Symposium (Am. Inst. Chem. Eng.), ser. 33, vol. 57, 1961, pp. 28–37.

SEIFERT, H. S.: Twenty-Five Years of Rocket Development. Jet Prop., vol. 25, no. 11, Nov. 1955.

SUTTON, GEORGE P.: Rocket Propulsion Elements. Second ed., John Wiley & Sons, Inc., 1956.

The Chemistry of Propellants. Combustion and Propulsion Researches and Reviews. AGARD, Pergamon Press, 1960.

Jet Propulsion Engines. Vol. XII of High Speed Aerodynamics and Jet Propulsion, Princeton Univ. Press, 1959.

Liquid Propellants Handbook, vols. 1 to 3, and LPIA Abstracts, 1958 to Present. Liquid Propellant Info. Agency, Appl. Phys. Lab., Johns Hopkins Univ.

Propellant Manual. SPIA/M–2, Feb. 1961, and SPIA Abstracts. Solid Propellant Info. Agency, Appl. Phys. Lab., Johns Hopkins Univ.

Rocket Motor Manual. SPIA/M–1, vols. 1 and 2, Sept. 1962, SPIA, Appl. Phys. Lab., Johns Hopkins Univ.

37. Fluid Physics of Liquid Propellants

By Donald L. Nored and Edward W. Otto

DONALD L. NORED, *an Aerospace Scientist at the Lewis Research Center, is engaged in program planning and design studies for pressurization systems and fluid components in the Apollo Propulsion Office. He has worked on advanced propulsion facility design and operation, high-energy-propellant rocket engine development, and vehicle systems studies. Mr. Nored received his B.S. degree in Chemical Engineering from Texas Technological College in 1955. He is a member of the American Rocket Society and the American Institute of Chemical Engineers and is a registered Professional Engineer of the State of Ohio.*

EDWARD W. OTTO *is Head of the Fluid Systems Section of the Lewis Research Center. He has specialized in propulsion systems dynamics and controls and is currently engaged in the study of the behavior of liquids in a zero-gravity environment. Mr. Otto is a graduate of Iowa State University, where he received his B.S. degree in Mechanical Engineering in 1944. He is a member of Pi Tau Sigma and Phi Kappa Phi.*

INTRODUCTION

The use of liquid propellants in chemical rocket engine propulsion systems, while quite common, has necessitated the solution of a number of problems peculiar to rocket vehicles. Two relatively new areas of application, however, have presented new fluid physics problems. These areas are (1) the use of cryogenic propellants in general and (2) the use of liquid propellants in a space vehicle. This discussion treats these two new areas of application by reviewing the various attendant problems and indicating the extent of present knowledge.

Figure 37–1, showing a typical liquid bipropellant rocket vehicle, indicates those areas directly concerned with the physics of the fluid systems. These fluid systems are composed of the tankage for the liquid propellants, associated internal baffles and diffusers, insulation surrounding the tanks, and the pressurization system. Also included are the necessary lines, control components, and heat exchangers. The problems existing in such systems may be divided into two categories: those pertaining to the powered phases of a mission and those pertaining to the coast phases. Pressurization and sloshing of propellants are the two problem

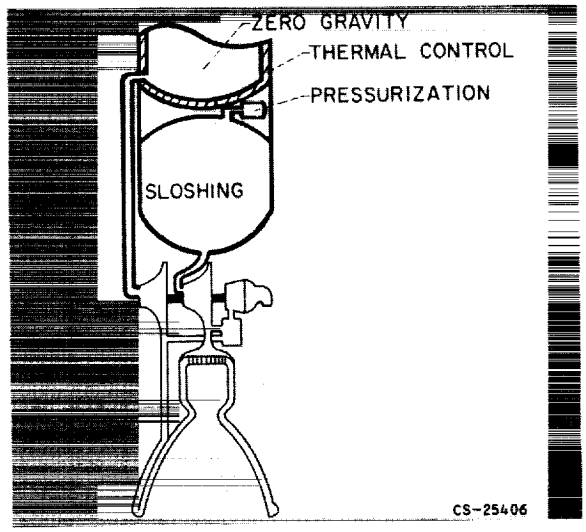

FIGURE 37–1.—Problem areas in typical liquid propellant rocket fluid systems.

areas of interest during the powered phases, while thermal control and effects of zero gravity are of interest during coast.

PRESSURIZATION

The first major problem area, pressurization, exists whether the vehicle is pressure-fed or pump-fed since a pressurization system of some kind will always be required. Such a pressurization system can become a large part of vehicle dry weight for those space vehicles utilizing cryogenic propellants for the following reasons:

(1) Liquid hydrogen has a low density, hence the tanks will be large, and a resultant large amount of pressurant will be required.

(2) There will be a drastic drop in the temperature of the incoming pressurizing gas; thus, the final gas density will be high, and even more gas will be required.

The largest problem encountered in the field of pressurization is the accurate prediction of pressurant requirements. Such prediction is difficult because of the complex transient physical and thermodynamic processes occurring within the propellant tank. These processes are shown in figure 37–2.

The heat-transfer processes of primary importance are the heat transferred to the walls, heat transferred to the liquid, and heat transferred to the ullage space vapor and gas by the incoming pressurizing gas. The mode of internal heat transfer to the walls and liquid is some form of free convection; thus, the geometry of the tank becomes important. The heat transferred to the ullage gas and vapor is dependent on the mixing occurring and hence is a function of diffuser design (i.e., inlet gas distribution), propellant vapor density changes, and pressurant density changes. Heat transfer from the external environment, from the wall to the liquid, and by axial conduction is generally quite small during the expulsion period but of extreme importance during coasting periods.

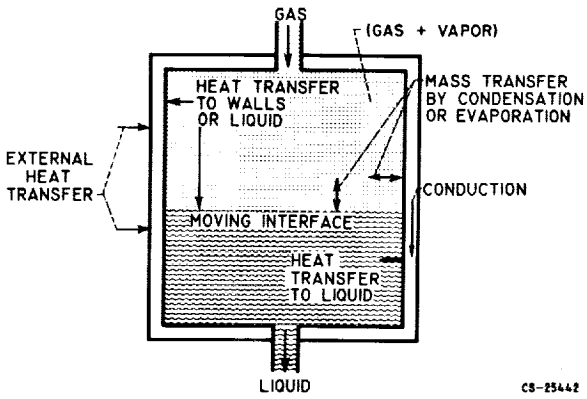

FIGURE 37–2.—Heat- and mass-transfer processes affecting pressurization during expulsion.

The mass transfer within the tank occurs by condensation and evaporation at the liquid interface and wall interface. Generally, it is assumed that mass transfer, while significant in small tanks, becomes quite small as tank size increases. Recent data taken on Saturn tanks, however, indicate that such mass transfer may be larger than is generally assumed. In any event, the analytical prediction of mass transfer is perhaps the most difficult task in determining pressurant requirements. The transient nature of the processes occurring, as well as the unknown pressurant and vapor distribution throughout the ullage space, are only two of the reasons for the task being difficult. Future mathematical models based on analytical studies must of necessity include considerations of mass transfer, with experimental tests being required to establish the actual magnitude and mode of such mass transfer, especially for large tanks.

Because of the transient nature of the various processes, with system parameters varying in both time and space, temperature stratification occurs during expulsion. The stratification within the liquid causes a warm layer of liquid to form at the interface, although the temperature of the bulk of the liquid remains relatively constant. Temperature stratification that occurs within the ullage space varies from the warm liquid temperature at the interface to the gas inlet temperature at the top of the tank. There are also concentration gradients throughout the ullage space of the inlet pressurant, pressurant used in previous expulsions, and propellant vapor. These gradients are dependent upon diffusion effects and degree of mixing, variables not subject to ready analysis, as well as history effects (i.e., time of pressurization prior to expulsion, heat transfer during coast,

venting during coast, pressurant added in previous firings of the engine system, etc.).

As can be appreciated, an analytical approach to the problem of predicting pressurant requirements is extremely difficult. In general, the variables affecting the heat- and mass-transfer processes, and thus influencing pressurant requirements, are (1) pressurant type and state, (2) propellant type and state, (3) propellant tank characteristics, (4) expulsion characteristics, (5) history of the tank and contents, (6) slosh, vortexing, and diffuser design, and (7) gravity field. Several methods have been advanced for predicting pressurant requirements; however, they are limited in application, particularly for space vehicles, either because of simplifying assumptions or because many of the variables are neglected. Better methods, of a more generalized nature and verified by representative experimental data, will be required in the future in order that realistic space vehicles may be designed.

Another problem concerning pressurization systems is the selection of a particular system. The general requirements for a pressurization system for a space vehicle always include: (1) lightweight and (2) high reliability, and depending upon the mission, may include (3) restart capability, (4) instant readiness, (5) long-term compatibility with the propellants, and (6) variable flow capability. Since a multitude of systems exist that potentially meet these requirements, some type of classification is required for the process of selection. If systems are classified according to source of pressurizing fluid, there are only four major classes. Roughly in order of decreasing system weight and increasing system complexity, the classes of systems are those that use

(1) Stored gases
(2) Evaporated propellants
(3) Evaporated nonpropellants
(4) Products of a chemical reaction

The first class is one of the most common, being used in some form in most of the present-day liquid-propellant rocket vehicles. Stored helium systems typical of this class have high reliability; compatibility is not a problem; and there is a backlog of experience on components. Some of the parameters influencing the weight of the system are: (1) storage temperature, (2) storage pressure, (3) type of gas expansion, and (4) material used for the storage tank.

The second class, using evaporated propellants, is the next most common type of system. This type of system has been used on several pump-fed vehicles where the liquid, usually liquid oxygen, is tapped off downstream of the pump, vaporized in some convenient heat exchanger, and then used to pressurize the propellant tank from which it was obtained. Systems for pressure-fed vehicles have not been developed to any extent, but they offer great potential in weight savings (especially for liquid hydrogen) and should be studied further.

Evaporated-nonpropellant systems, the third class, have not been tested extensively. Indeed, only two types of systems could be contemplated as being useful for cryogenics, those using liquid helium and liquid nitrogen. Each of these has certain disadvantages, however, that would generally preclude their use.

The last class, systems using products of a chemical reaction, perhaps offers the greatest potential in future weight savings. Gas generators to generate gaseous products for use in pressurizing storable propellant tanks have been developed and flown. Another method, having undergone a small amount of testing recently, involves the injection of a hypergolic (spontaneously ignitible) fluid into one of the propellant tanks. This permits the reaction to occur within the tank. The method is attractive for the liquid-hydrogen tank in particular, since vaporized liquid hydrogen, if obtainable, has a lower gas density than the reaction products. Although the method is basically simple, it does present problems of control, especially of temperature.

The selection of a system from the four classes for a particular space vehicle depends not only on the requirements just discussed, but also on the tradeoffs involved with other systems. The development of the more advanced systems, particularly in the areas of controls, heat exchangers, components, and materials, will be desirable in order to give a more valid basis for the tradeoffs involved.

SLOSHING OF PROPELLANTS

The second major problem area influencing the use of liquid propellants in rocket vehicles is propellant sloshing. Oscillations may result, for example, from the attitude control system and can exert forces and moments on the vehicle that cause a shift in the center of gravity. Figure 37–3 shows a schematic of a vehicle undergoing sloshing. The propellant sloshing exerts side forces which, at a maximum, may reach a force approximately equal to one-quarter of the apparent weight of the propellant. These side forces not only increase structural loads on the tankage and supports, but also require thrust-vector control from the rocket engine. In extreme cases, critical disturbances to the stability of the vehicle may occur. Furthermore, when sloshing occurs, the pressurization gas entering the tank may be cooled more rapidly, and thus more gas would be required. Still another effect might be the exposure of the outlet to vapor. This would result in vapor entering the flow systems, where it could have disastrous effects. The alleviation or elimination of sloshing is, therefore, extremely desirable.

Figure 37–4 shows the slosh-force parameter as a function of the frequency parameter for a half-full spherical tank. These parameters are nondimensionalized and are independent of tank size or density of the liquid. The solid curve represents the theoretical results for unrestricted nonviscous sloshing. The effects of various methods of slosh control are shown, and they are best compared at the first natural frequency at which the largest slosh forces arise. The first natural frequency is the point at which the excitation and fundamental frequencies of the contained liquid are equal.

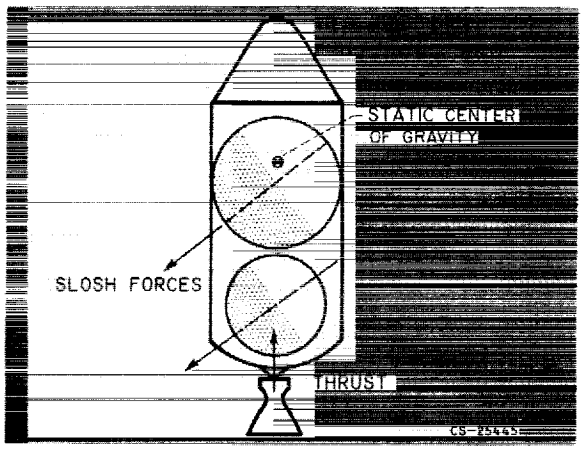

FIGURE 37–3.—Forces exterted on vehicle during sloshing.

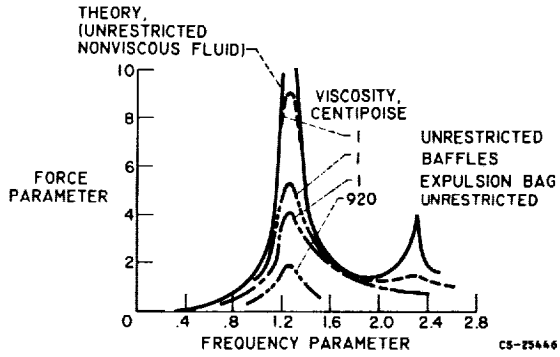

FIGURE 37–4.—Effects of control devices on slosh forces in half-full spherical tank.

The most common method to date of controlling sloshing is by placing baffles within the tank. While effective, these are seen to be the worst of three available methods. The second method utilizes a continuous surface film, such as obtained by expulsion bags or diaphragms. This method is more effective than baffles, but involves problems of compatibility, leakage, venting, fabrication, and other mechanical difficulties, particularly for large tanks. Since expulsion bags also permit displacement of liquids under zero gravity, however, such an approach has been used for relatively small-scale propellant tanks—slosh control being gained as a secondary feature. The third method is the most effective and involves increasing the viscosity of the liquid; for the case shown in figure 37–4, the viscosity was increased from 1 to 920 centipoise. Successful attempts have been made at increasing the viscosity of so-called Earth storable propellants by gelling the propellants and making a thixotropic material out of the liquid; however, very little progress has been made in such gelling for cryogenic propellants. Indeed, the gelling of cryogenics remains as one of the few fields in which large advances may still be made.

THERMAL CONTROL OF PROPELLANTS

The third major problem area is thermal control of the propellants. For cryogenic liquids the incoming thermal energy must be minimized since such heat input will cause propellant heating, vaporization, and a resulting loss of propellant by venting. Unless these losses are small, the potential advantages of using cryogenic propellants will vanish.

The sources of propellant heating may be either internal or external with respect to the space vehicle, as indicated by figure 37–5. The space vehicle is assumed to comprise four sections. The payload section contains the instrumentation and guidance equipment and must be maintained at a temperature on the order of 520° R. The liquid-oxygen section requires a temperature of approximately 163° R, while the liquid-hydrogen tank must be maintained at approximately 37° R; the engine temperature will depend on the type of engine system. These temperatures may vary somewhat, depending upon the pressure of the propellant, the type of instrumentation, and the specific design of the vehicle, but the relative order of magnitude will remain the same.

Heating due to internal sources is caused by thermal radiation between the various components of the vehicle and by conduction through propellant lines and structural supports. The possible external sources of heat are the sun, the planets and their moons, and the galaxies. Heat is transferred between the vehicle and these sources solely by thermal radiation. The largest external heat flux encountered by a space vehicle within our solar system is usually that which originates from the sun. The heat flux received from a planet results partly from planetary radiation and partly from reflected solar radiation. This planetary heat flux becomes greater as the planet is approached, and, in some cases, could become of the same order of magnitude as the solar heat flux. Galactic heating is negligibly small and is usually ignored.

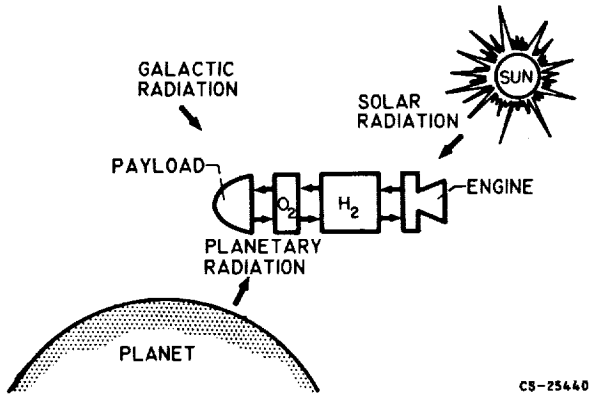

FIGURE 37–5.—Sources of heat input to cryogenic vehicle in space.

In general, interstage conduction is controlled by using minimum areas and low-conductivity materials for all components attached to the tank. Thus, the major problem of heat input is one of proper control of thermal radiation due both to internal and external sources. Various methods of control of thermal radiation are available, and they may be classified as orientation, coatings, and insulations.

By proper orientation of the vehicle certain sections can shade other sections. For example, the payload could be pointed toward the sun, thus acting as an effective external sun shadow shield for the rest of the vehicle. Also, arrangement is important since the oxygen tank could act as a shadow shield for the hydrogen tank, protecting it against internal thermal radiation from the payload. In any case, however, some other method of thermal radiation control must still be employed since such arrangement or orientation will leave at least one section at too high a temperature for effective use.

Various inorganic or organic coatings are available which, by the proper balance of emissivity and absorptivity, permit some equilibrium temperature to be attained by the surface on which the coating is applied. The lowest temperature obtainable, however, by presently available coatings, is still much higher than the temperatures of the cryogenic liquids. Hence, while useful, coatings will not alone provide the proper temperature environment and must be supplemented by other methods of thermal radiation control.

The best means of control is the use of insulations. Figure 37–6 shows a comparison of various insulations that are useful for space vehicles. The product of apparent thermal conductivity and density is used as the means of

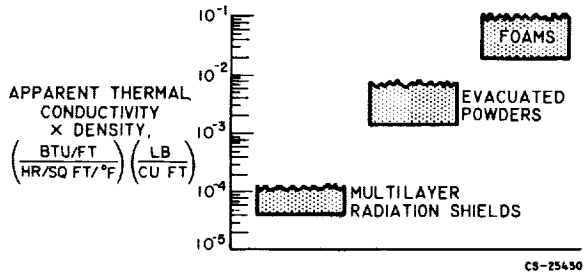

FIGURE 37-6.—Comparison of insulations for space applications.

comparison since this product arises when the basic heat-transfer equation for conduction is modified to reflect insulation weight. Optimum insulation occurs when this product is a minimum. The apparent thermal conductivity is determined from measurements of the net heat flux across a thickness of insulation, and thus includes conduction, radiation, and convection if applicable. Foams are typical of those insulations that restrict the flow of heat primarily by means of low thermal conduction alone. Evacuated powder-type insulations not only have low conduction and very little convection, but also reduce the radiant energy transfer and thus result in a much lower apparent thermal conductivity than foams. At present, however, the best of the insulations consists of parallel, thermally isolated, reflected shields. Such shields are more effective than powders in reducing radiant heat transfer, and thus are better insulations for thermal control of propellants under space conditions. If close together, these shields are commonly called foils. The so-called superinsulations consist of reflective foils separated by very low-conduction materials.

In use, foams are relatively easy to apply to the vehicle tanks but give high weights of insulation required. The powders require a rigid jacket around the tank for correct placement, which increases the weight and causes problems of settling and the occurrence of voids. Foils also have an installation problem, as compressive loads reduce their efficiency. Trade-offs, therefore, between the various insulations must be made for each particular mission, as well as for the proper use of each of the methods of thermal control. At present, however, the effects of compressive loads, and techniques of design, such as fastening, supporting, and evaluation, require more work before valid trade-offs may be performed.

EFFECTS OF ZERO GRAVITY

The final problem area to be discussed concerns the effects of weightlessness (i.e., zero gravity) on the liquid propellants. Weightlessness will be encountered by space vehicles during orbital or space missions, and a knowledge of the final equilibrium liquid-vapor interface configuration will be needed to solve the problems of effective tank venting and proper pump inlet design. Furthermore, a knowledge of the modes of heat transfer to stored propellants during periods of weightlessness will also be needed.

Control of Interface

For effective control of the liquid-vapor interface the various forces predominating in a zero-gravity environment must be understood. Such forces are generally intermolecular in nature; that is, they are relatively small, are exerted over a short range, and are independent of the gravitational field. One such force that should persist in zero gravity is the surface tension of the liquid, or, a property associated with surface tension, the contact angle at which the liquid meets the solid surface (measured in the liquid). Another consideration for a zero-gravity environment actually is based on the observed characteristic of systems to assume a state of minimum energy when external forces are removed. This would suggest that the interfaces, if free to move, would assume some

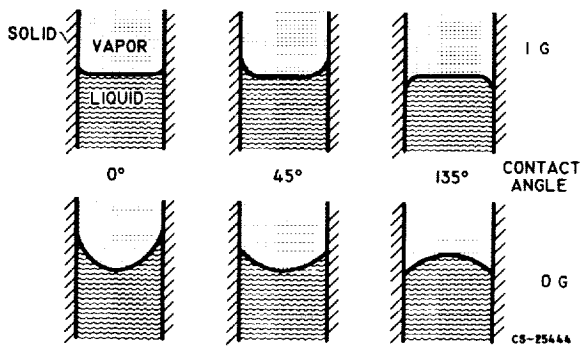

FIGURE 37-7.—Interface configurations in cylindrical container as function of gravity field and contact angle.

spherical shape, this being the shape representative of minimum energy.

Figure 37–7 indicates the effect of combining these two conditions for liquid in a cylindrical container. Both the 1-g and zero-g configurations are shown, for a range of contact angles. For the 1-g case the contact angle of the liquid is observed in the meniscus at the liquid-solid interface. Upon entering the zero-gravity state, the contact angle will be preserved, and the liquid-vapor interface, being free to move, will adjust itself until a constant curvature surface is reached. In an enclosed container, of course, the actual shape of the liquid surface would not only be determined by contact angle preservation and considerations of minimization of energy, but also by the shape of the container and the amount of liquid in the container.

To verify the reasoning used in this analysis many experimental tests have been conducted at the Lewis Research Center, primarily in a 2.25-second-free-fall drop tower. These tests have verified the predictions in every detail. Selected photographs taken from motion-picture data (using high-speed photography) for a typical test drop are shown in figure 37–8. This figure shows a 100-milliliter glass sphere with a liquid- to tank-volume ratio of 40 percent. The liquid in this case is ethyl alcohol, which has a contact angle of zero and is thus representative of the cryogenic fluids. The photographs represent the conditions at 1 g and the equilibrium conditions for zero g. It can be seen that, at 1 g, the alcohol rests in a pool at the bottom of the sphere. The liquid surface is essentially flat. The meniscus is concave, and the liquid contacts the wall at an angle of 0°. During the zero-g period, the liquid begins to rise along the wall, and the liquid surface becomes curved. At the equilibrium condition the result is a completely wetted tank wall with a spherical vapor bubble in the interior of the liquid.

The results of the experimental studies, as previously indicated, have tended to verify the prediction that the total surface energy is minimized in zero gravity. In order to provide further verification, a definitive analytical model was studied. This model used a geometry consisting of a hollow tube suspended

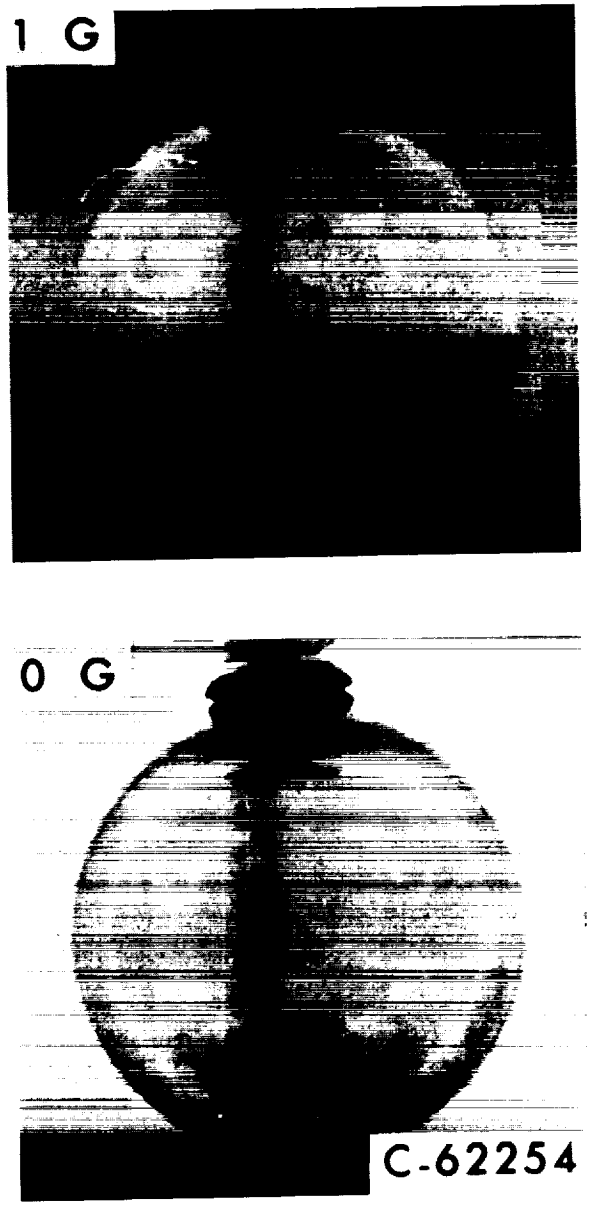

FIGURE 37–8.—Interface configurations of wetting liquid in spherical container at normal gravity and during weightlessness. Tank 40 percent full.

within a cylindrical tank, aligned with the vertical axis, and being open to the liquid at both top and bottom. An analysis of this configuration, solving for the minimization of surface energy, indicated that for liquids with contact angles less than 90° the liquid will rise in the tube if the tube radius is less than one-half the tank radius, will remain level if the tube radius is equal to one-half the tank radius, and

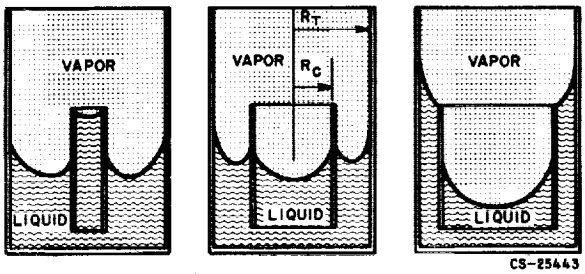

(a) $R_c < \frac{1}{2} R_T$. (b) $R_c = \frac{1}{2} R_T$. (c) $R_c > \frac{1}{2} R_T$.

FIGURE 37–9.—Effect of tube radius on interface configuration for wetting liquid in cylindrical container.

will fall if the tube radius is greater than one-half the tank radius.

Experimental tests have been conducted with wetting liquids in a similar geometry, in which the tube radius was varied and the direction of liquid motion was observed as the experiment was subjected to zero gravity. Results of these experiments are summarized schematically in figure 37–9 for a liquid with a contact angle of 0°. Sketches of the interface configurations are shown after equilibrium conditions in zero gravity have been reached. Three tube radii (R_c) were used, being respectively less than, equal to, and greater than one-half the tank radius (R_T). These experiments verified the previous analysis in every detail and provided proof that the solid-liquid-vapor system will tend to assume a configuration of minimum free surface energy when placed in a weightless environment.

APPLICATIONS

As a result of these fundamental studies, it appears that the tank systems can be designed by using suitable internal baffling to position the liquid-vapor interface properly. The principal requirements of an interface control system in a propellant tank are that it maintain a quantity of liquid over the pump inlet, and, if venting is necessary, that it maintain the main ullage volume over the vent. The capillary tube geometry employed in the minimum-surface-energy studies appears to provide a satisfactory interface configuration in that it locates liquid over the pump inlet if such a pump inlet is placed at the bottom of the capillary tube and vapor over the vent if the vent is located above the tube.

The configuration of the liquid-vapor interface in zero gravity, obtained with a standpipe geometry for two orientations of the container, is shown in figure 37–10. This figure shows a 100-milliliter glass sphere with a liquid- to tank-volume ratio of 30 percent. Again ethyl alcohol (containing a dye for ease of photography) is used in order to duplicate cryogenic liquids having a contact angle of zero. The capillary tube (or standpipe) has a tube diameter of 33 percent of sphere diameter and a relative height of 60 percent. The photographs in figure 37–10(a) indicate the ability of the liquid to fill the standpipe and the vapor to form over the vent (if located above the standpipe) for the case in which the sphere enters zero gravity at an angle of 0° between the gravity vector and the axis of the standpipe. Figure 37–10(b) is similar, except that the sphere enters zero gravity at an angle of 90°, and again the ability to position the liquid and vapor bubble is shown. Such ability, however, is very time dependent, and for low fillings a relatively long period of time is required to properly position the vapor bubble after zero gravity has been entered at a high angle to the initial gravity vector.

The standpipe geometry encounters difficulties in positioning the vapor bubble over the vent at high fillings, however, when the vapor bubble is small. If the standpipe is made relatively high, there is danger that the bubble could become trapped in the annular space following an adverse acceleration. A geometry that avoids entrapment of the vapor bubble and urges it to the vicinity of the vent or, conversely, pumps the liquid to the bottom of the tank would be desirable. Liquid can be pumped by capillary forces from one end of a tank to the other if tapered geometry is used and suitable return paths are provided. This principle may be employed to overcome some of the difficulties encountered with standpipes at high fillings. The application of this principle to a spherical tank is shown in figure 37–11. The tapered section is formed in this case by offsetting a second sphere within the first. The geometry is now such that the vapor bubble obtains its

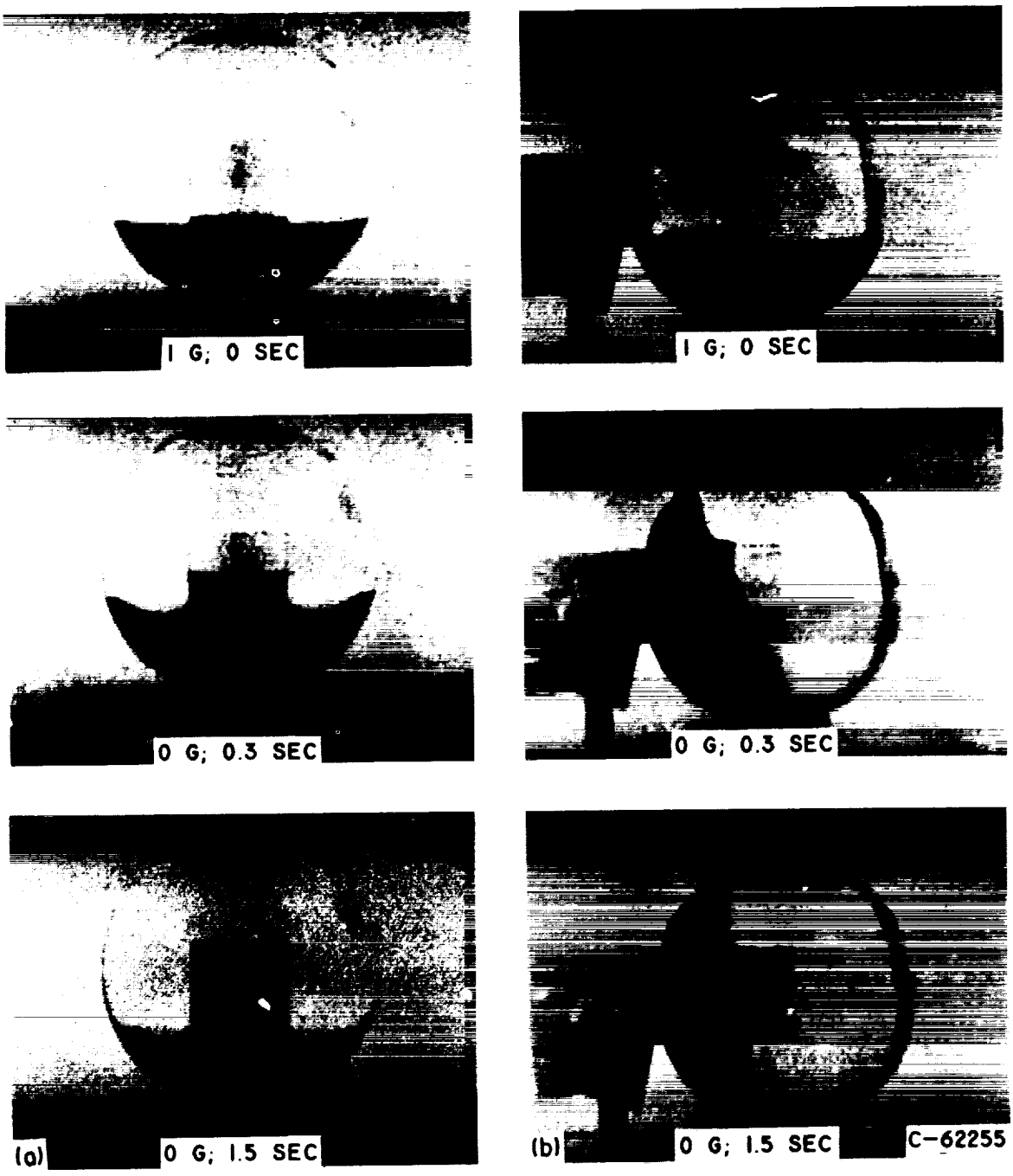

(a) Initial position, 0° between gravity vector and standpipe.
(b) Initial position, 90° between gravity vector and standpipe.

FIGURE 37-10.—Movement of wetting liquid in capillary tube ullage control geometry.

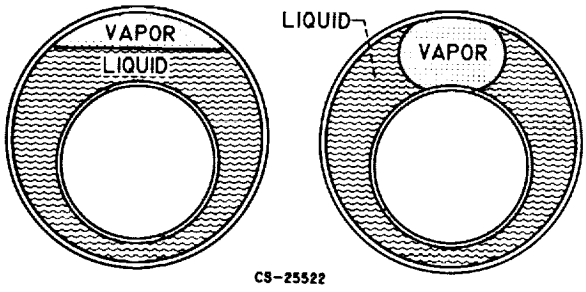

(a) 1-g configuration.
(b) Zero-g configuration.

FIGURE 37-11.—Application of tapered section principle to spherical tank.

most nearly spherical shape under the vent but cannot become completely spherical even for fillings of 95 percent. The result is the movement of the bubble to the vent from any starting position. The ability of this geometry to move the vapor bubble is shown in figure 37-12; the vapor bubble is initially 90° away from the vent but is pumped toward the vent by capillary action when zero gravity is entered. In this experiment, the outer sphere has a volume of 100 milliliters. The inner sphere is 60 percent of the diameter of the outer sphere, which forms a tapered annular section around the inner sphere. The liquid is again ethyl alcohol, and the liquid- to tank-volume ratio is 95 percent.

While the experiments to date have indicated that the liquid-vapor interface can be adequately controlled, two questions remain to be answered. The scaling parameter of time must be further studied, and the amount of acceleration to disrupt a surface under zero gravity must be known. Acceleration disturbances (crew movement, orientation maneuver, etc.) may cause the liquid and vapor to be improperly oriented, and thus an unknown length of time may be required for proper positioning.

Heat Transfer

Another problem on which further research is needed is that of heat transfer under weightless conditions. The mechanism of heat input to a tank under space conditions corresponds to that of a classical pool-boiling situation, the various regions of which are shown in figure 37-13 for a 1-g field. The coordinates are heat

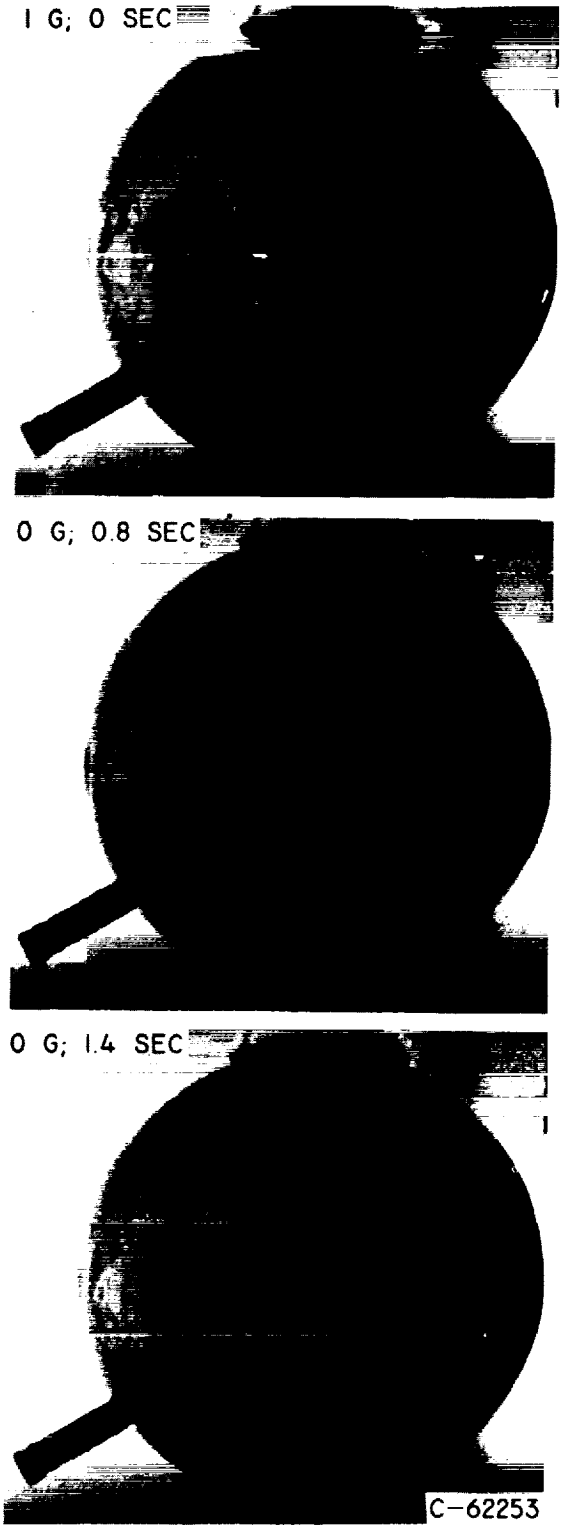

FIGURE 37-12.—Movement of vapor bubble in tapered-section ullage control geometry. Initial position, 90° from vent; wetting liquid.

flux plotted as a function of temperature difference.

The heat-transfer regions start with conduction at very low flux, and, as flux is increased, progress through convection and nucleation, and finally, at very high flux, to the mechanism of film boiling. The regions of convection and nucleation may be substantially affected by the loss of gravity. Convection currents should certainly be absent in a zero-gravity environment, although residual currents might persist for some time; however, the nucleation picture is less clear. The velocity of bubbles through the liquid depends on the gravity field. If the velocity becomes zero because of loss of buoyancy, the nucleation region may be replaced by a film mechanism of boiling. This situation would be predicted by a proposed nucleation concept that is gravity dependent. A nucleation model has been proposed, however, which is independent of gravity in that bubbles are removed from the surface by a flow field set up around the bubble because of its rate of expansion. If this model is correct, the nucleation region should be relatively unaffected by a zero-gravity environment, and this region would probably extend down to cover the convection region.

A series of experiments using liquid hydrogen has been performed by General Dynamics/Astronautics in which the heat transfer in the nucleate range as a function of temperature difference was measured at 1–g and zero–g conditions. Results of this study are shown in figure 37–14. These results indicate that zero

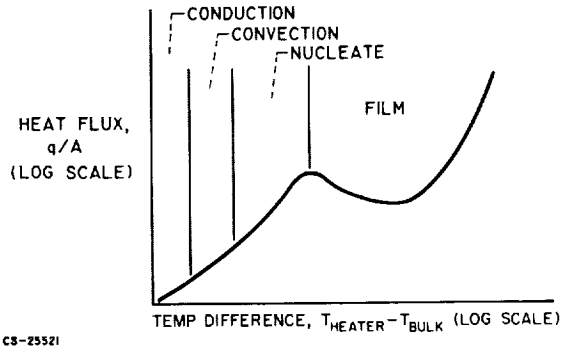

FIGURE 37–13.—Typical pool boiling charcteristics for 1–g field.

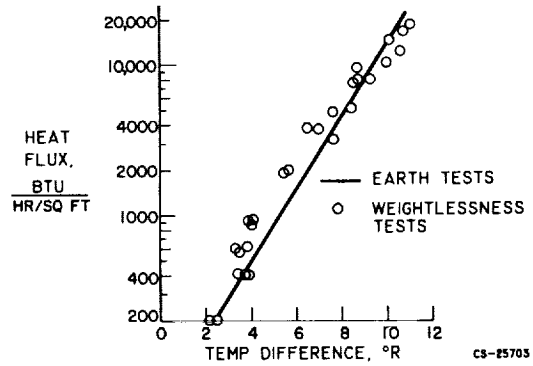

FIGURE 37–14.—Comparison of 1–g and zero-g liquid-hydrogen heat-transfer characteristics for nucleate boiling range. Small, directly heated metal specimens in pool of liquid hydrogen.

gravity has little effect on heat transfer in the nucleate region, which supports the nucleation model that is independent of gravity. The scaling parameter of time, however, among others, is probably quite important in these experiments, and much more work in this area is needed in order to extend our knowledge of heat transfer processes to the zero-gravity situation.

The primary effect of the heat-transfer mechanism for cryogenic liquids is the pressure rise within the container. This problem could be serious in a long term coasting situation. In a normal gravity field, convection currents and high bubble velocities cause most of the heat to be delivered to the gas space, which causes an abnormal pressure rise and thus excessive venting. The heat sink capacity of the liquid, which is considerable in the case of cryogenic propellants, is lost. In a zero-gravity field, if the conduction and nucleation regions are replaced by a film process, again most of the heat will be delivered to the gas, and the heat sink capacity of the liquid will be lost. If the gravity-independent nucleation concept is correct, however, the nucleation continues, but at reduced bubble velocity. Thus more time is available for bubbles to condense as they move through the liquid, more heat is delivered to the liquid, and a lower pressure rise results. Since the available data tend to support the gravity-independent nucleation concept, it would appear that less pressure rise will be experienced in zero gravity than under normal

gravity. The magnitude of this effect is still relatively unknown, however, and warrants further study.

CONCLUDING REMARKS

In summary, four problem areas primarily involving the use of cryogenic liquids in space vehicles have been briefly discussed. Some answers exist for these areas, but further work, of both a fundamental and an applied nature, is required. In particular, more detailed information is needed on the physical and thermodynamic properties for the liquids of interest. Furthermore, the areas of heat and mass transfer need better definition under conditions peculiar to a space vehicle.

The problem areas of fluid physics as outlined are not the only areas of interest today, and, as space flights become more ambitious, even more areas requiring study will appear. Indeed, the successful operation of space vehicles must depend upon future solutions to these and other problems.

BIBLIOGRAPHY

Pressurization

ARPACI, V. S., and CLARK, J. A.: Dynamic Response of Fluid and Wall Temperatures During Pressurized Discharge for Simultaneous, Time-Dependent Inlet Gas Temperature, Ambient Temperature, and/or Ambient Heat Flux. Vol. 7 of Advances in Cryogenic Eng., K. D. Timmerhaus, ed., 1961, p. 419.

ARPACI, V. S., CLARK, J. A., and WINER, W. O.: Dynamic Response of Fluid and Wall Temperatures During Pressurized Discharge of a Liquid from a Container. Vol. 6 of Advances in Cryogenic Eng., K. D. Timmerhaus, ed., Plenum Press, 1960, p. 310.

BOWERSOCK, D. C., GARDNER, R. W., and REID, R. C.: Pressurized Transfer of Cryogenic Liquids. Vol. 4 of Advances in Cryogenic Eng., K. D. Timmerhaus, ed., Plenum Press, 1958, p. 342.

BOWERSOCK, D. C., and REID, R. C.: An Analytical Method for Estimating Gas Requirements in the Pressurization and Transfer of Cryogenic Fluids. Vol. 6 of Advances in Cryogenic Eng., K. D. Timmerhaus, ed., Plenum Press, 1960, p. 261.

CLARK, J. A., VAN WYLEN, G. J., and FENSTER, S. K.: Transient Phenomena Associated with the Pressurized Discharge of a Cryogenic Liquid from a Closed Vessel. Vol. 5 of Advances in Cryogenic Eng., K. D. Timmerhaus, ed., Plenum Press, 1959, p. 467.

COXE, E. F., and TATOM, J. W.: Analysis of the Pressurizing Gas Requirements for an Evaporated Propellant Pressurization System. Vol. 7 of Advances in Cryogenic Eng., K. D. Timmerhaus, ed., Plenum Press, 1961, p. 234.

FENSTER, S. K., VAN WYLEN, G. J., and CLARK, J. A.: Transient Phenomena Associated with the Pressurization of Liquid Nitrogen Boiling at Constant Heat Flux. Vol. 5 of Advances in Cryogenic Eng., K. D. Timmerhaus, ed., Plenum Press, 1959, p. 226.

GLUCK, D. F., and KLINE, J. F.: Gas Requirements in Pressurized Transfer of Liquid Hydrogen. Vol. 7 of Advances in Cryogenic Eng., K. D. Timmerhaus, ed., Plenum Press, 1961, p. 219.

KAPLAN, C.: Selection of Pressurization System for Storable Liquid Propellant Rocket Engines. ARS Jour., vol. 31, no. 6, June 1961, pp. 786–793.

NEIN, M. E., and HEAD, R. R.: Experiences with Pressurized Discharge of Liquid Oxygen from Large Flight Vehicle Propellant Tanks. Vol. 7 of Advances in Cryogenic Eng., K. D. Timmerhaus, ed., 1961, p. 244.

SCHMIDT, A. F., PURCELL, J. R., WILSON, W. A., and SMITH, R. V.: An Experimental Study Concerning the Pressurization and Stratification of Liquid Hydrogen. Vol. 5 of Advances in Cryogenic Eng., K. D. Timmerhaus, ed., Plenum Press, 1959, p. 487.

SUTTON, J. F., et al.: Main Propellant Tank Pressurization System Study and Test Program. Rep. ER-4728, Lockheed Aircraft Corp., Marietta, Georgia, Feb. 1961.

VAN WYLEN, G. J., FENSTER, S. K., MERTE H., JR., and WARREN, W. A.: Pressurized Discharge of Liquid Nitrogen from an Uninsulated Tank. Vol. 4 of Advances in Cryogenic Eng., K. D. Timmerhaus, ed., Plenum Press, 1958, p. 395.

WALSH, THOMAS J., HIBBARD, R. R., and ORDIN, PAUL M.: Dillution of Liquid Oxygen when Nitrogen is Used for Pressurization. NACA RM E58A03a, 1958.

Anon.: Main Propellant Tank Pressurization System Study and Test Program. Rep. ER-5238, Lockheed Aircraft Corp., Marietta, Georgia, Aug. 1961.

Anon.: Main Propellant Tank Pressurization System Study and Test Program. Rep. ER-5296, vol. III. Lockheed Aircraft Corp., Marietta, Georgia, Dec. 1961.

Sloshing

ABRAMSON, H. NORMAN, and RANSLEBEN, GUIDO E., JR.: A Note on the Effectiveness of Two Types of Slosh Suppression Devices. Tech. Rep. 6, Southwest Res. Inst., June 15, 1959.

ABRAMSON, H. NORMAN, and RANSLEBEN, GUIDO E., JR.: A Note on Wall Pressure Distributions During Sloshing in Rigid Tanks. Tech. Rep. 5, Southwest Res. Inst., June 15, 1959.

ABRAMSON, H. NORMAN, and RANSLEBEN, GUIDO E., JR.: Simulation of Fuel Sloshing Characteristics in Missile Tanks by Use of Small Models. Tech. Rep. 7, Southwest Res. Inst., Apr. 25, 1960.

BAUER, HELMUT F.: Fluid Oscillations in a Circular Cylindrical Tank. Rep. DA-TR-1-58, Army Ballistic Missile Agency, Apr. 18, 1958.

BAUER, HELMUT F.: Fluid Oscillation in a Cylindrical Tank with Damping. Rep. DA-TR-4-58, Army Ballistic Missile Agency, Apr. 23, 1958.

BAUER, HELMUT F.: Propellant Sloshing. Rep. DA-TR-18-58, Army Ballistic Missile Agency, Nov. 5, 1958.

BUDIANSKY, BERNARD: Sloshing of Liquids in Circular Canals and Spherical Tanks. Jour. Aero/Space Sci., vol. 27, no. 3, Mar. 1960, pp. 161–173.

COLE, HENRY A., JR., and GAMBUCCI, BRUNO J.: Tests of an Asymmetrical Baffle for Fuel-Sloshing Suppression. NASA TN D-1036, 1961.

LAMB, HORACE: Hydrodynamics. Sixth ed., Dover Pub., 1945.

LEONARD, H. WAYNE, and WALTON, WILLIAM C., JR.: An Investigation of the Natural Frequencies and Mode Shapes of Liquids in Oblate Spheroidal Tanks. NASA TN D-904, 1961.

MCCARTY, JOHN LOCKE, LEONARD, H. WAYNE, and WALTON, WILLIAM C., JR.: Experimental Investigation of the Natural Frequencies of Liquids in Toroidal Tanks. NASA TN D-531, 1960.

MCCARTY, JOHN LOCKE, and STEPHENS, DAVID G.: Investigation of the Natural Frequencies of Fluids in Spherical and Cylindrical Tanks. NASA TN D-252, 1960.

O'NEILL, J. P.: An Experimental Investigation of Sloshing. STL-TR-59-0000-09960, Space Tech. Labs., Inc., Mar. 4, 1960.

STEPHENS, DAVID G., LEONARD, H. WAYNE, and SILVERIA, MILTON A.: An Experimental Investigation of the Damping of Liquid Oscillations in an Oblate Spheroidal Tank With and Without Baffles. NASA TN D-808, 1961.

STOFAN, ANDREW J., and ARMSTEAD, ALFRED L.: Analytical and Experimental Investigation of Forces and Frequencies Resulting from Liquid Sloshing in a Spherical Tank. NASA TN D-1281, 1962.

STOFAN, ANDREW J., and PAVLI, ALBERT J.: Experimental Damping of Liquid Oscillations in a Spherical Tank by Positive-Expulsion Bags and Diaphragms. NASA TN D-1311, 1962.

Thermal Control

BALLINGER, J. C.: Environmental Control Study of Space Vehicles, Pt. 1. Rep. ERR-AN-004, General Dynamics/Astronautics, Mar. 9, 1960.

BALLINGER, J. C.: Environmental Control Study of Space Vehicles, Pt. 2. Rep. ERR-AN-004, General Dynamics/Astronautics, Nov. 1, 1960.

BALLINGER, J. C.: Environmental Control Study of Space Vehicles, Pt. 2. Supp. A, Rep. ERR-AN-016, General Dynamics/Astronautics, Dec. 31, 1960.

BALLINGER, J. C.: Environment Control Study of Space Vehicles, Pt. 2, Supp. B, Rep. ERR-AN-016, General Dynamics/Astronautics, Jan. 20, 1961.

BALLINGER, J. C.: Environmental Control Study of Space Vehicles, Pt. 3. Rep. ERR-AN-051, General Dynamics/Astronautics, Dec. 31, 1960.

BURRY, R. V., and DEGNER, V. R.: Liquid-Propellant Storage Evaluation for Space Vehicles. Fourth Symposium on Ballistic Missile and Space Tech., Aug. 1959.

CHRISTIANSEN, R. M., HOLLINGSWORTH, M., JR., and MARSH, H. N., JR.: Low Temperature Insulating Materials. 1959 Cryogenic Eng. Confer., Sept. 2–4, 1959.

CRAMER, KENNETH R.: Orbital Storage of Cryogenic Fluids. TN 58-282, WADC, Oct. 1958.

CORNOG, ROBERT: Temperature Equilibria in Space Vehicles. Proc. Am. Astronautical Soc., Western Regional Meeting, Aug. 18–19, 1958.

CUNNINGHAM, F. G.: Earth Reflected Solar Radiation Input to Spherical Satellites. NASA TN D–1099, 1962.

CUNNINGHAM, F. G.: Power Input to a Small Flat Plate from a Diffusely Radiating Sphere, with Application to Earth Satellites. NASA TN D–710, 1961.

DRISCOLL, D. G.: Cryogenic Tankage for Space Flight Applications. 1959 Cryogenic Eng. Conf., Sept. 2–4, 1959.

GAZLEY, CARL, JR., KELLOGG, W. W., and VESTINE, E. H.: Space Vehicle Environment. Jour. Aero/Space Sci., vol. 26, no. 12, Dec. 1959.

GLASER, PETER E., ed.: Aerodynamically Heated Structures. Prentice-Hall, Inc., 1962.

GOLDMAN, D. T., and SINGER, S. F.: Radiation Equilibrium and Temperature. Proc. of VII Int. Astronautical Cong. (Rome), Sept. 17–22, 1956.

HELLAR, GERHARD: Thermal Control of the Explorer Satellites. Paper 834–59, ARS, 1959.

HNILICKA, MILO P.: Engineering Aspects of Heat Transfer in Multilayer Reflective Insulation and Performance of NRC Insulation. 1959 Cryogenic Eng. Conf., Sept. 2–4, 1959.

JOHNSON, FRANCIS S.: Satellite Environment Handbook. Stanford Univ. Press, 1961.

JOHNSON, FRANCIS S.: The Solar Constant. Jour. of Meteorology, vol. 11, no. 6, Dec. 1954, pp. 431–439.

KREITH, F.: Radiation Heat Transfer and Thermal Control of Spacecraft. Pub. 112, Eng. Exp. Station, Oklahoma State Univ., Apr. 1960.

OLIVIER, J. R., and DEMPSTER, W. E.: Orbital Storage of Liquid Hydrogen. NASA TN D–559, 1961.

SCOTT, RUSSELL B.: Cryogenic Engineering. D. Van Nostrand Co., Inc., 1959.

SMOLAK, G. R., and KNOLL, R. H.: Cryogenic Propellant Storage for Round Trips to Mars and Venus. Paper 60–23. Inst. Aero. Sci., 1960.

SMOLAK, GEORGE R., KNOLL, RICHARD H., and WALLNER, LEWIS E.: Analysis of Thermal-Protection Systems for Space-Vehicle Cryogenic-Propellant Tanks. NASA TR R–130, 1962.

WOOD, GEORGE P., and CARTER, ARLEN F.: The Design Characteristics of Inflatable Aluminized-Plastic Spherical Earth Satellites with Respect to Ultraviolet, Visible, Infrared and Radar Radiation. Paper 59–AV–38, ASME, 1959.

Zero Gravity

ADAM, NEIL KENSINGTON: The Physics and Chemistry of Surfaces. Oxford Univ. Press, 1941.

ADAMSON, ARTHUR W.: Physical Chemistry of Surfaces. Intersci. Pub., 1960. Aerophysics Group: June–August Progress report for the Combined Laboratory and KC–135 Aircraft Zero-G Test Program. Rep. AE61–0871, Convair Astronautics, Sept. 5, 1961.

ALEXANDER, A. E.: Surface Chemistry. Longmans, Green, and Co., 1951.

BARTWELL, F. E.: Wetting of Solids by Liquids. Colloid Chem., vol. III, Chem. Catalog Co., Inc., 1931.

BENEDIKT, E. T.: Dynamics of a Liquid Spheroid Under the Action of Cohesive Forces. Rep. ASRL–TM–60–10, Norair Div., Northrop Corp., Sept. 1960.

BENEDIKT, E. T.: General Behavior of a Liquid in a Zero or Near Zero Gravity Environment. Rep. ASG–TM–60–9Z6, Norair Div., Northrop Corp., May 1960.

BENEDIKT, E. T.: Scale of Separation Phenomena in Liquids Under Conditions of Nearly Free Fall. ARS Jour., vol. 29, no. 2, Feb. 1959, pp. 150–151.

BERNETT, M. K., and ZISMAN, W. A.: Relation of Wettability by Aqueous Solutions to the Surface Constitution of Low-Energy Solids. Jour. Phys. Chem., vol. 63, no. 8, Aug. 1959, pp. 1241–1246.

BIKERMAN, J. J.: Surface Roughness and Contact Angle. Jour. Phys. and Colloid Chem., vol. 54, no. 5, May 1950, pp. 653–658.

BRAZINSKY, IRVING, and WEISS, SOLOMON: A Photographic Study of Liquid Hydrogen at Zero Gravity. NASA TN D–1107, 1961.

BURDON, R. S.: Surface Tension and the Spreading of Liquids. Cambridge Univ. Press (London), 1940.

CALLAGHAN, EDMUND E.: Weightlessness. Machine Design, vol. 34, no. 24, Oct. 11, 1962, pp. 156–161.

CASSIE, A. B. D.: Contact Angles. Discussions of Faraday Soc., no. 3, 1948, pp. 11–16.

DUPRE, ATHANASE: Memoirs of the Mechanical Theory of Heat. Nos. 5, 6, and 7, Ann. Chim. et Phys., 1866–1868.

FORSTER, H. K., and ZUBER, N.: Growth of a Vapor Bubble in a Superheated Liquid. Jour. Appl. Phys., vol. 25, Apr. 1954, pp. 474–478.

FOWKES, FREDERICK M., and HARKINS, WILLIAM D.: The State of Monolayers Adsorbed at the Interface Solid-Aqueous Solution. Jour. Am. Chem. Soc., vol. 62, no. 12, Dec. 1940, pp. 3377–3386.

GAUSS, CARL FRIEDERICH: Principia Generalia Theoriae Figurae Fluidorum in Statu Aequilibrii. Gottingen, 1830.

GERATHEWOHL, SIEGFRIED J.: Zero-G Devices and Weightlessness Simulators. Pub. 781, Nat. Acad. Sci.-Nat. Res. Council, 1961.

GIBBS, J. WILLARD: Collected Works. Vol. 2. Longmans, Green, and Co., 1928.

GLASSTONE, SAMUEL: Textbook of Physical Chemistry. Second ed., D. Van Nostrand Co., Inc., 1946, pp. 481–483.

GOOD, ROBERT J., and GIRIFALCO, L. A.: A Theory for Estimation of Surface and Interfacial Energies. III. Estimation of Surface Energies of Solids from Contact Angle Data. Jour. Phys. Chem., vol. 64, no. 5, May 1960, pp. 561–565.

GOODRICH, F. C.: The Mathematical Theory of Capillarity, I; II; III. Proc. Roy. Soc. (London), ser. A, vol. 260, no. 1303, Mar. 21, 1961, pp. 481–509.

GREGG, S. J.: Hystersis of the Contact Angle. Jour. Chem. Phys., vol. 16, no. 5, May 1948, pp. 549–550.

GURNEY, C.: Surface Forces in Liquids and Solids. Proc. Phys. Soc. (London), sec. A, no. 358, vol. 62, Oct. 1, 1949, pp. 639–648.

HARKINS, WILLIAM D.: The Physical Chemistry of Surface Films. Reinhold Pub. Corp., 1952.

HARKINS, WILLIAM D., and LOESER, E. H.: Surfaces of Solids. XIX Molecular Interactions Between Metals and Hydrocarbons. Jour. Chem. Phys., vol. 18, no. 4, Apr. 1950, pp. 556–560.

JONES, EDWARD W.: What Does "Weightlessness" Really Mean? Space/Aero., vol. 38, no 5, Oct. 1962, pp. 65–67.

KOENIG, FREDERICK O.: On the Thermodynamic Relation Between Surface Tension and Curvature. Jour. Chem. Phys., vol. 18, no. 4, Apr. 1950, pp. 449–459.

LANGMUIR, IRVING: The Constitution and Fundamental Properties of Solids and Liquids, I. Jour. Am. Chem. Soc., vol. 38, no. 11, Nov. 1916, pp. 2221–2295.

LAPLACE, PIERRE SIMON: Mecanique Celeste, Supplement to Tenth Book, 1806.

LI, T.: Cryogenic Liquids in the Absence of Gravity. Vol. 7 of Advances in Cryogenic Eng., K. D. Timmerhaus, ed., Plenum Press, 1962, pp. 16–23.

LI, TA: Liquid Behavior in a Zero-G Field. Rep. AE 60–0682, Convair-Astronautics, Aug. 1960.

MCNUTT, JAMES E., and ANDES, GEORGE M.: Relationship of the Contact Angle to Interfacial Energies. Jour. Chem. Phys., vol. 30, no. 5, May 1959, pp. 1300–1303.

MERTE, H., and CLARK, J. A.: Boiling Heat Transfer Data for Liquid Nitrogen at Standard and Near-Zero-Gravity. Vol. 7 of Advances in Cryogenic Eng., K. D. Timemrhaus, ed., 1961, p. 546.

MILLER, N. F.: The Wetting of Steel Surfaces by Esters of Unsaturated Fatty Acids. Jour. Phys. Chem., vol. 50, no. 4, July 1946, pp. 300–319.

NEINER, J. J.: The Effect of Zero Gravity on Fluid Behavior and System Design. TN 59–149, WADC, Apr. 1949.

PARTINGTON, J. R.: An Advanced Treatise on Physical Chemistry. Vol. II. Longmans, Green, and Co., 1951, pp. 134–207.

PETRASH, DONALD A., ZAPPA, ROBERT F., and OTTO, EDWARD W.: Experimental Study of the Effects of Weightlessness on the Configuration of Mercury and Alcohol in Spherical Tanks. NASA TN D–1197, 1962.

PLATEAU, J. A. F.: Statique Experimentale et Theorique des Liquides. 1873.

POISSON, SIMEON DENIS: Nouvelle Theorie de L'Action. 1831.

RAYLEIGH: Collected Scientific Papers. Vol. VI. Cambridge Univ. Press (London), 1920.

REYNOLDS, W. C.: Hydrodynamic Consideration for the Design of Systems for Very Low Gravity Environments. Tech. Rep. LG–1, Dept. Mech. Eng., Stanford Univ., Sept. 1961.

REYNOLDS, WILLIAM C.: Behavior of Liquids in Free Fall. Jour. Aero/Space Sci., vol. 26, no. 12, Dec. 1959, pp. 847–848.

ROHSENOW, W. M.: A Method of Correlating Heat-Transfer Data for Surface Boiling Liquids. Trans. ASME, vol. 74, 1952, p. 969.

SCHOLBERG, HAROLD M., and WETZEL, W. W.: Some Observations on the Theory of Contact Angles. Jour. Chem. Phys., vol. 13, no. 10, Oct. 1945, p. 448.

SHAFRIN, ELAINE G., and ZISMAN, WILLIAM A.: Constitutive Relations in the Wetting of Low Energy Surfaces and the Theory of the Retraction Method of Preparing Monolayers. Jour. Phys. Chem., vol. 64, no. 5, May 1960, pp. 519–524.

SHERLEY, J. E., and MERINO, F.: The Final Report for the General Dynamics/Astronautics Zero-G Program Covering the Period from May 1960 Through March 1962. Rep. AY62–0031, General Dynamics/Astronautics, Aug. 15, 1962.

SHERLEY, JOAN: Evaluation of Liquid Behavior in a Zero-G Field Using Free Floating Technique. Convair-Astronautics, 1960.

SHUTTLEWORTH, R.: The Surface Tension of Solids. Proc. Phys. Soc. (London), sec. A, vol. 63, no. 365, May 1, 1950, pp. 444–457.

SHUTTLEWORTH, R., and BAILEY, G. L. J.: The Spreading of a Liquid Over a Rough Solid. Discussions of Faraday Soc., no. 3, 1948, pp. 16–21.

SIEGEL, ROBERT: Transient Capillary Rise in Reduced and Zero-Gravity Fields. Paper 60-WA–201, ASME, 1960.

STEINLE, HANS: Heat Transfer in a Zero-G Field. Convair-Astronautics, 1960.

USISKIN, C. M., and SIEGEL, R.: An Experimental Study of Boiling in Reduced and Zero Gravity Fields. Paper 60–HT–10, ASME-AIChE, 1960.

WASHBURN, E. ROGER, and ANDERSON, ELMER A.: The Pressure Against Which Oils Will Spread on Solids. Jour. Phys. Chem., vol. 50, no. 5, Sept. 1946, pp. 401–406.

YARNOLD, G. D.: Understanding Surface Tension. Contemporary Phys., vol. 1, no. 4, Apr. 1960, pp. 267–275.

YARNOLD, G. D., and MASON, B. J.: The Angle of Contact Between Water and Wax. Proc. Phys. Soc., sec. B, vol. 62, pt. 2, Feb. 1949, pp. 125–128.

YARNOLD, G. D., and MASON, B. J.: A Theory of the Angle of Contact. Proc. Phys. Soc., sec. B, vol. 62, pt. 2, Feb. 1949, pp. 121–125.

YOUNG, THOMAS: Essay on the Cohesion of Fluids. Roy. Phil. Trans., Dec. 20, 1805, pp. 65–87.

YUST, WALTER, ed.: Surface Tension. Encyclopaedia Britannica, Inc., vol. 21, 1947, pp. 593–602.

38. New Problems Encountered With Pumps and Turbines

By Melvin J. Hartmann and Calvin L. Ball

MELVIN J. HARTMANN *is Head of the Pump Section of the Fluid System Components Division of the NASA Lewis Research Center. He has conducted and supervised research in the field of turbomachinery. Mr. Hartmann earned his B.S. degree in Mechanical Engineering from the University of Nebraska in 1944. He is a member of the Institute of the Aerospace Sciences.*

CALVIN L. BALL, *Aerospace Scientist at the NASA Lewis Research Center, is conducting research on turbomachinery, primarily involving pumps for cryogenic fluids that are applicable to rocket engines. Mr. Ball attended Michigan College of Mining and Technology and received his B.S. degree in Mechanical Engineering in 1956. He is a member of the American Society of Mechanical Engineers.*

INTRODUCTION

As the missions in the space program become more difficult, a wide range of new requirements are placed on all components of both chemical and nuclear rocket engine systems. The advent of manned space flight has resulted in stringent requirements on the reliability of all rocket components in an effort to eliminate catastrophic engine failure. The trend toward larger booster engines and higher engine operating pressures has required increased size and pressure producing capability of the turbopump units. The smaller thrust engines used to provide thrust in space as well as in landing and rendezvous maneuvers require that the turbopumps perform satisfactorily over a wide range of thrust levels (engine throttlability) and, in addition, provide multiple restart capability. The pumping systems for these engines must respond nearly instantaneously to demands of the control system even though the propellants may have been stored for long periods in the space environment. For some of the new engines there is the requirement that the pump accept the propellants from the tank at or near their boiling points.

Further complexities exist in the development of pumping machinery for future rocket engines. Statistics have indicated that about one-third of the effort in a rocket engine development program is devoted to the turbopump. Because the development of the turbopump is a long process, it is often necessary to establish many of the engine parameters long before turbopump test data are available. If the turbopump does not achieve the performance assumed in establishing engine performance parameters, a complete redesign involving expensive and critical time delays may be necessary. In the past this problem has been handled by overdesigning the turbopump to meet possible deficiencies. Because of the new requirements placed on the turbopump, design parameters are being pushed closer and closer to limitations set by the present state of technology. Therefore, there no longer exists sufficient margin for overdesigning to satisfy possible deficiencies showing up in the development phase. As a result, it is necessary to improve pump design techniques to meet the increased requirements with assurance that a suitable turbopump will result.

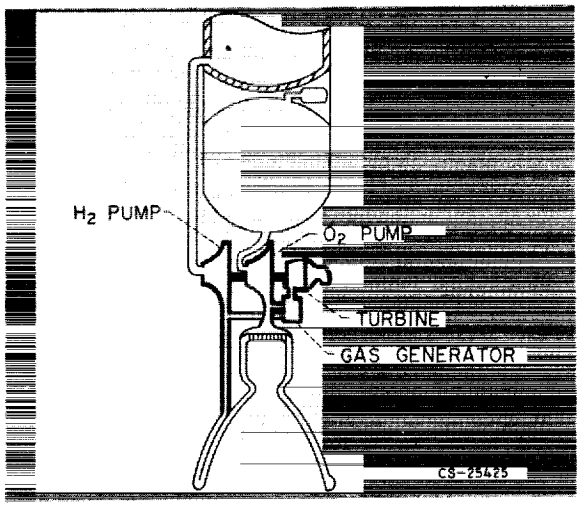

FIGURE 38–1.—Chemical-rocket pumps and turbine.

From figure 38–1, some of the general functions and requirements of the turbopump in a chemical rocket system may be inferred. In general, the propellant must be moved from the low-pressure tank to the high-pressure engine system. The propellants are usually stored at low pressures for minimum tank weight, and boiling or cavitation may occur in the fluid system wherever the pressure is further reduced by velocity increase. The pump must be capable of ingesting such vapor and still increasing the pressure of the propellants. Furthermore, the propellants must be delivered to the engine without pressure or flow fluctuations that could result in a thrust fluctuation or possible destructive engine instabilities. The power for pumping the propellant must be developed by a turbine. The exhaust from the turbine develops a relatively small thrust, and thus the flow through the turbine must be minimized to avoid a sizable reduction in engine specific impulse, the energy release in pound-seconds per pound of propellant.

This paper covers three topics pertinent to the turbopump:

(1) Pumping under cavitating conditions
(2) Flow stability in high-pressure pumps
(3) Turbine drives with high-energy propellants

The discussion mainly concerns hydrogen or hydrogen-oxygen turbines and pumps. It is applicable, in general, to modern turbomachinery for all rocket propellants and to both chemical and nuclear rocket systems.

PUMPING UNDER CAVITATING CONDITIONS

In general, when the pump must operate with the inlet fluid very near the boiling condition, vapor forms in the pump inlet. The formation of vapor bubbles and their subsequent collapse as the fluid is exposed to boiling or vapor pressure in low-pressure regions of the flow is referred to as cavitation. The inlet portion of the pump must be capable of increasing the pressure to suppress the boiling even when the flow contains some vapor. Several methods of approaching the cavitation problem are illustrated in figure 38–2. In the upper left sketch of figure 38–2 an inducer stage is added to the pump. This stage is designed to operate under cavitating conditions and increases the pressure sufficiently above the vapor pressure so that the main-stage pump is not affected by cavitation. This can also be thought of as a prepumping stage raising the pressure in the line ahead of the main pump rather than increasing the pressure in the entire tank to suppress boiling. The lower left sketch illustrates an inducer stage ahead of an axial-flow pump. The upper right sketch illustrates a pump in which the inducer is integral with the main stage of the pump. In this type of pump the design must avoid interactions between the

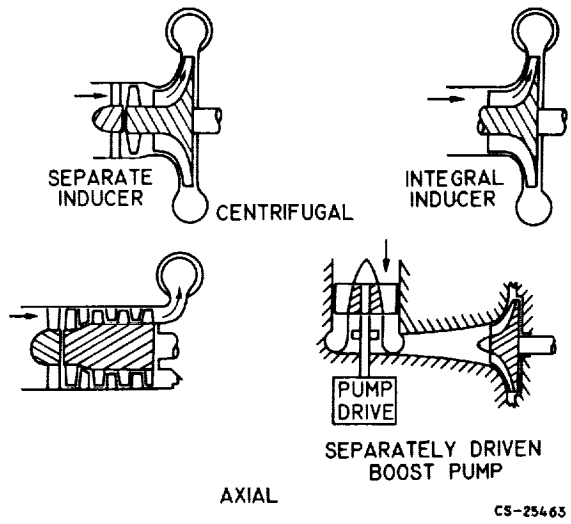

FIGURE 38–2.—Pump and inducer configurations.

cavitation and the blade loading necessary to obtain high pump pressure rises. In each of these three configurations either a separate inducer or an inducer portion of the pump is utilized to obtain energy addition or pressure rise even under cavitating conditions. In each case the inducer is operated at pump speed. If the inlet conditions are too close to fluid vapor pressure to obtain the necessary suction performance in this manner, it is necessary to add a low-speed booster pump ahead of the high-speed pump. Such a configuration is shown in the lower right sketch of figure 38–2. The booster pump may be driven by a variety of devices, including gears, an electric motor, and gas or hydraulic turbines. Whether a high-speed or low-speed cavitating pump inducer is utilized, it is necessary to understand the vapor formation within the pump rotor and to find ways to minimize the formation of vapor and the effect of these vapor formations on the pressure production capability of the pump.

Vapor forms when the low-pressure regions of a pump rotor are at or below fluid vapor pressure. The low-pressure regions exist in vortices formed with tip or corner flows and on the low-pressure portion of the pump blades. Figure 38–3 shows two pump blades rotating in the downward direction with the relative flow entering from the left. The high- and low-pressure portions of the blade are indicated by plus and minus signs. The integrated difference in these pressures reflects the level of energy addition to the pumped fluid. As a result of this pressure difference there is a flow in the clearance space, as indicated in the lower left sketch of figure 38–3. At the intersection of the crossflow and the through flow, a vortex is formed. The center of this tip vortex forms a line at an angle to the inducer blade depending on the relative velocity of the through flow and the crossflow. The center of this vortex is a low-pressure region in which vapor first forms. As the inlet pressure is lowered further, vapor forms in the region of the crossflow and closes in the region between the blade and the tip vortex and thus completely obscures the view of the vaporous regions on the low-pressure surface of the inducer blade.

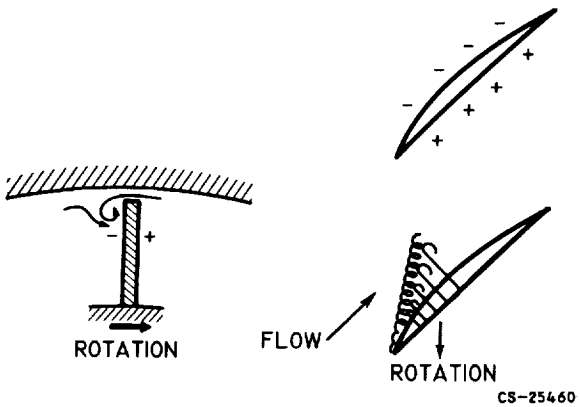

FIGURE 38–3.—Vortex formed because of flow through tip clearance space.

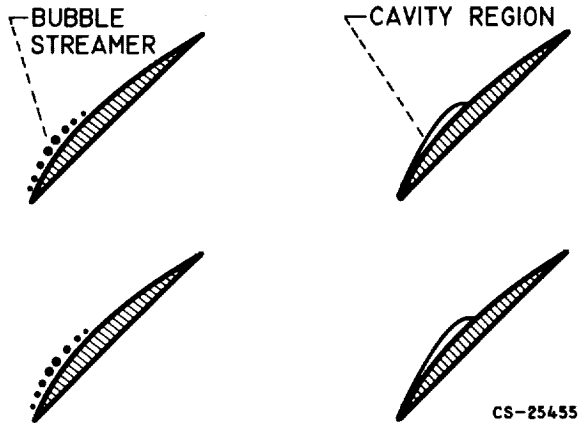

FIGURE 38–4.—Vapor formation at blade surface.

The vapor formation on the blade surface can only be observed by viewing the inducer from the upstream direction. In this manner a view under the tip vortex can be obtained. The blade surface cavitation forms in one of two configurations shown in figure 38–4. The right sketch illustrates a cavity region forming on the blade leading edge and closing on the low-pressure surface of the blade. This type of vapor formation occurs when vapor pressure occurs at the blade leading edge. When the leading-edge shape is optimized so that fluid vapor pressure first occurs some small distance back from the blade leading edge, streamers of bubbles occur along the low-pressure surface of the blade. This latter type of vapor configuration is illustrated in the left sketch of figure 38–4. Under normal operating conditions very little difference in performance exists as a result of the type of blade surface cavitation, but rather is determined by the degree of cavitation.

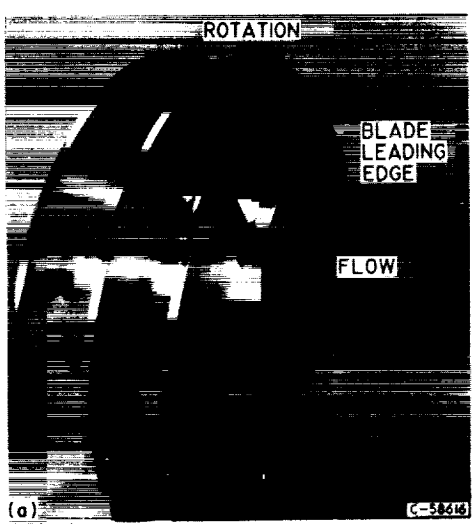
ROTATION
BLADE LEADING EDGE
FLOW
(a)
C-58618

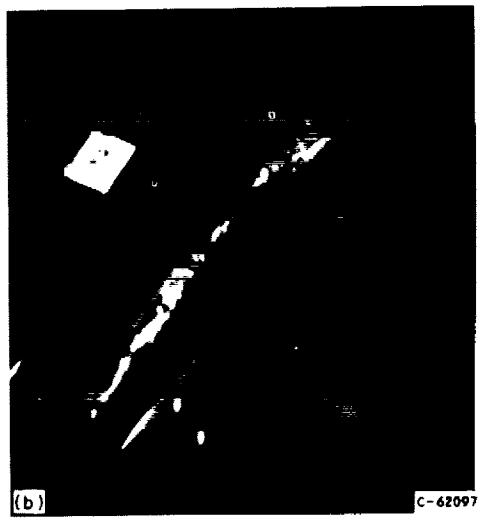
(b)
C-62097

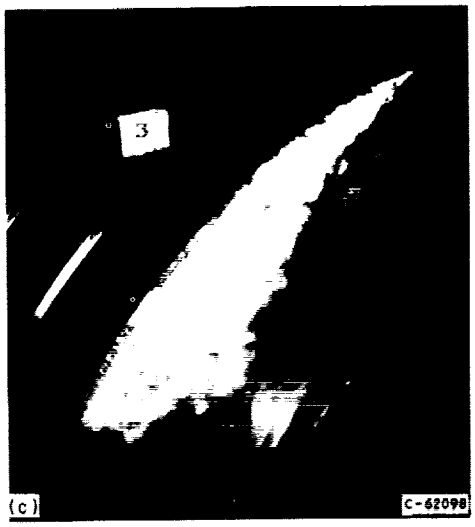
3
(c)
C-62098


(d)
C-62099


(e)

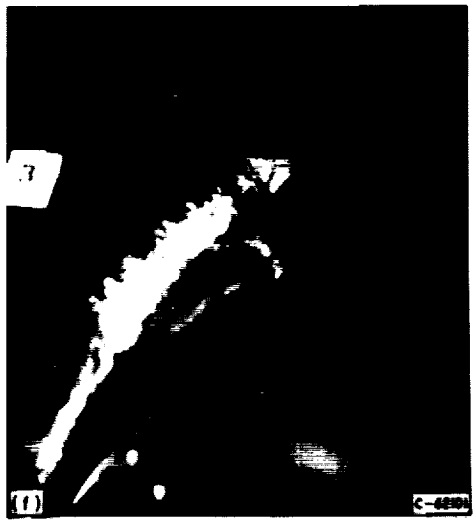
7
(f)

In either case, the vapor region is very close to the blade surface, and the blade surface pressure is very nearly fluid vapor pressure.

Basic research on cavitation can be done most easily and inexpensively in water with verification tests using the actual propellants. A series of photographs illustrating a pump inducer and the various types of vapor formation that are observed in water is shown in figure 38–5. The helical inducer that was operated in the Lewis water tunnel with a transparent housing is shown in figure 38–5(a). The directions of rotation and flow are indicated in the photograph. The orientation of the inducer blades to the flow is similar in the following five photographs, selected to illustrate the cavitation configuration discussed in connection with the sketches in figures 38–3 and 38–4.

The photograph shown in figure 38–5(b) illustrates the formation of cavitation vapor in the center of the tip vortex. The side of the inducer blade being viewed is the low-pressure surface. Thus, the cross-flow is normal to the blade toward the lower right direction, and it causes the tip vortex to form as shown. Over the forward portion of the blade some vapor forms in the crossflow, and the tip vortex appears nearly attached to the blade. Vapor is then confined to a narrow region of the vortex. When this process is viewed as a movie, there is a slight oscillatory motion of the tip vortex. Figure 38–5(c) illustrates the tip vortex and crossflow vapor formation as the inlet pressure is lowered toward fluid vapor pressure. The blade tip and the tip vortex form the edges of the vaporous region. Under these conditions the vapor extends to only about ¼ inch from the outer housing. Any surface cavitation that may exist on the low-pressure surface of the blade is not visible unless the camera is placed in a more forward position so that a view under this tip cavitation can be obtained.

←

(a) Orientation of helical inducer.
(b) Formation of tip vortex cavitation.
(c) Cavitation in tip vortex and crossflow region.
(d) Cavitation appearing as streamers on blade low-pressure surface.
(e) Blade surface cavity at moderate inlet pressure.
(f) Blade surface cavity at lower inlet pressure.

FIGURE 38–5.—Visual studies of cavitation on pump inducer in Lewis water tunnel.

Figure 38–5(d) was selected to show the formation of streamers of vapor bubbles on the low-pressure surface of the pump inducer blade. (White tufts of yarn used to indicate tip eddy flows are shown on the inside of the transparent housing. These yarn tufts are not significant to this discussion and should not be of concern.) The streamers of bubbles appear to start at various points on the blade surface some distance behind the blade leading edge and exist at all radii. The number of streamers and the length of the streamers increase as the inlet pressure is lowered toward fluid vapor pressure. When streamer cavitation is viewed as a movie, streamers seem to appear and disappear at random, even though overall cavitation conditions appear to be constant.

Figures 38–5(e) and (f) were selected to illustrate a cavity region on the low-pressure surface of the pump inducer blade. The cavity begins at the blade leading edge and extends some distance along the blade. Lowering the inlet pressure toward fluid vapor pressure increases the length of the surface cavity. The surface of the cavity is "dimpled" in such a manner as to reflect light as bright points. The closure of the cavity also appears very bright because of the light reflection. When surface cavitation is viewed as a movie, the cavity closure point is noted to oscillate slightly forward and backward along the blade. With either type of surface cavitation the vapor formation is confined to a relatively narrow region from the blade suction surface with an estimated thickness comparable to blade thickness.

It is necessary to relate the vapor formation as inlet pressure is lowered toward fluid vapor pressure to the blade pressure distributions that control the energy addition to the pumped fluid. The sketch in figure 38–6 shows two blades moving downward with the relative flow from the lower left. The torque force being exerted on the fluid is related to the summation of the pressure difference on the high- and low-pressure blade surfaces. In this sketch a vaporous region is shown to exist on the low-pressure surface of the blade. Tip vortex cavitation is not shown since this constitutes a blockage effect on the through flow rather than a major effect on the blade pressure distribution (especially if the

666582 O—62——3

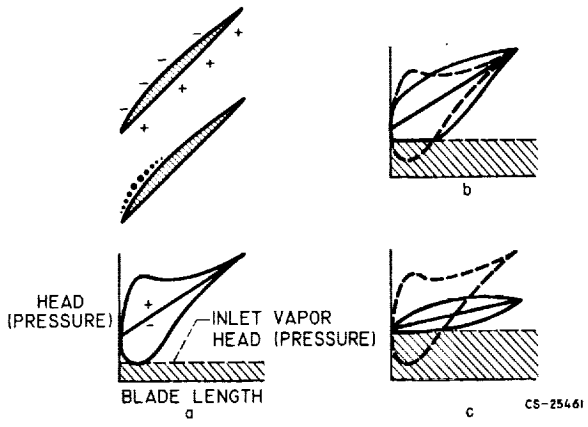

FIGURE 38-6.—Effect of cavitation on blade pressure distribution.

flow some small distance away from the blade tip is considered). The pressure distribution along the length of an inducer blade is sketched in figure 38-6(a). The mean pressure line at the inlet represents the inlet static pressure. The large pressure difference (high- to low-pressure blade surface) near the inlet is due to some angle of incidence between the inlet flow and blade mean angle. The pressure difference gradually decreases as the mean pressure approaches the discharge pressure. The cross-hatched region is the region below fluid vapor pressure. Pressure distributions of this general nature were utilized for pump inducer blades, and performance was not affected when the lowest blade surface pressure was at vapor pressure. In fact, in operation the inlet pressure can be lowered so that the indicated low-pressure point will be well below vapor pressure (assuming that the pressure distribution remains the same) before changes in performance are experienced. As the inlet pressure is lowered, the portion of the pressure distribution curve that would fall below the fluid vapor pressure line (as indicated by dashed lines in fig. 38-6(b)) probably does not exist. If the pump inducer is to continue to deliver the fluid to the discharge pressure, it is necessary for the pressure difference over the blade to increase in the rearward portion of the blade (solid lines), and for the total pressure loading to be sufficient to achieve the required head rise. Thus the inducer can continue to maintain the discharge pressure or head rise as long as the overall pressure loading can be maintained by redistribution rearward as the inlet pressure is lowered toward vapor pressure. This process can continue as long as the pressure gradient at the rear of the low-pressure blade surface can be achieved. When the fluid can no longer be delivered at the desired discharge pressure, the energy addition (area within the pressure loading diagram) decreases. This condition is illustrated in figure 38-6(c), and under these conditions the inducer will produce only a small head rise. The original or noncavitating blade pressure distribution is shown as a dotted line in figures 38-6 (b) and (c). The area of the pressure loading distributions represented by the solid line of figure 38-6(b) is meant to be essentially the same as that shown by the dotted curve. It should be noted that vapor formation just begins at the inlet pressure shown in figure 38-6(a) and that the length of vapor formation will increase from figure 38-6(b) to 38-6(c), as noted in figure 38-5.

The pressure loading diagrams can be related to pump inducer performance by comparison with figure 38-7. In this figure the head developed is plotted against the head above vapor pressure at the suction side of the pump. Condition A, where vapor first occurs on the inducer blade, on the solid curve exists at a sizable pressure above vapor pressure. It can be noted that tip vortex cavitation exists at inlet pressures well above point A. The vapor cavity continues to grow without affecting the inducer head produced as the inlet pressure is

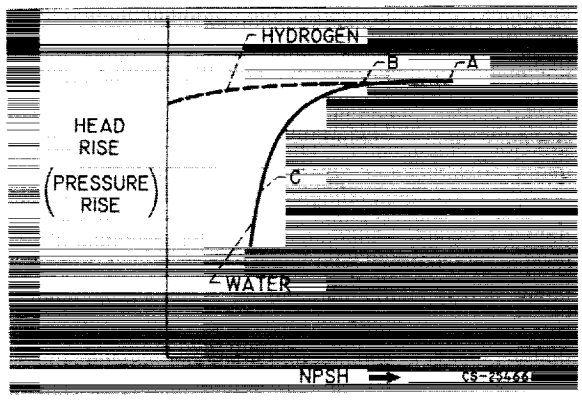

FIGURE 38-7.—Cavitation performance of pump inducer in water and in liquid hydrogen.

lowered to B. At lower inlet pressures corresponding to point C the pump inducer head rise falls off very rapidly. From the comparison it is concluded that the flow model description is suitable for inducers operating in water (solid line in fig. 38–7).

The cavitation performance of a given inducer in hydrogen may be vastly different from that obtained in water, as indicated by figure 38–7. As the inlet pressure was lowered at some point, the inducer head developed in water dropped off rather rapidly. In hydrogen, however, the head produced did not decrease drastically, even though the inlet pressure was reduced to vapor pressure (NPSH=0). An additional concept must be introduced into the blade loading diagram considerations to account for this large fluid property effect encountered with liquid hydrogen. These concepts are illustrated in figure 38–8. The sketch on the left shows the pressure distribution previously discussed at an inlet pressure just above that at which a performance loss would be experienced. It is believed that this is the type of performance encountered with water. The inlet static pressure is shown slightly higher than the inlet fluid vapor pressure. The inlet head, or total head, must be higher to account for the fluid velocity head at the pump inlet. (The term NPSH, inlet head above inlet fluid vapor pressure, is usually used to describe the inlet performance and is indicated in fig. 38–8.) On the other hand, other fluids, such as hydrogen, indicate a marked tendency to maintain some of the pressure loading below the inlet vapor pressure level. Several possible effects can occur to allow this low-pressure region to exist:

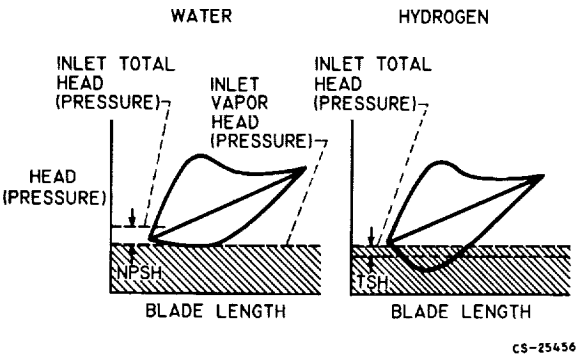

FIGURE 38–8.—Fluid property effects on blade-loading distribution.

(1) lower local fluid vapor pressure as a result of temperature drop due to fluid evaporation, (2) vapor and liquid with relatively similar densities and thus a relatively large pressure gradient that can be supported by a vaporous region, (3) fluid tension effects that retard the tendency to cavitate, and (4) rates of phase change relatively different between fluids.

One or more of these effects or others not indicated may occur to allow the blade pressure to drop below the fluid inlet vapor pressure. The net result is that the inlet pressure can be lowered further without experiencing a loss in head producing capability. The right sketch in figure 38–8 illustrates a case where the tank head and vapor pressure are coincidental. The amount that the inlet pressure can be lowered without reaching the limiting pressure gradient or the effectiveness of the pressure diagram that must exist below the inlet vapor pressure is a result of the thermodynamic properties of the fluid and thus is termed thermodynamic suppression head (TSH), as illustrated in figure 38–8. It is likely that the TSH effects are present in all fluids, but they are relatively small in water and relatively large in a fluid such as hydrogen. It may be feasible to incorporate the TSH effect into the equations for suction specific speed S_s and blade operating cavitation number k in the following manner:

Suction specific speed:

$$S_s=\frac{N\sqrt{Q}}{(\mathrm{NPSH})^{3/4}}\approx\frac{N\sqrt{Q}}{(\mathrm{NPSH}+\mathrm{TSH})^{3/4}}$$

where N is rotational speed in rpm, and Q is the flow rate in gallons per minute.

Effective cavitation number:

$$k=\frac{h_s-h_{vp}}{1/2\rho(V_1')^2}\approx\frac{h_s-h_{vp}+\mathrm{TSH}}{1/2\rho(V_1')^2}$$

where h_s and h_{vp} are the fluid static head and fluid vapor head at the inlet, respectively, and $1/2\rho(V_1')^2$ is the inlet relative velocity head.

It can be noted that for the performance produced in hydrogen as shown in figure 38–7 the suction specific speed term is infinity and the cavitation number becomes zero or negative, none of which are meaningful unless appropriate fluid property effects (TSH) are included.

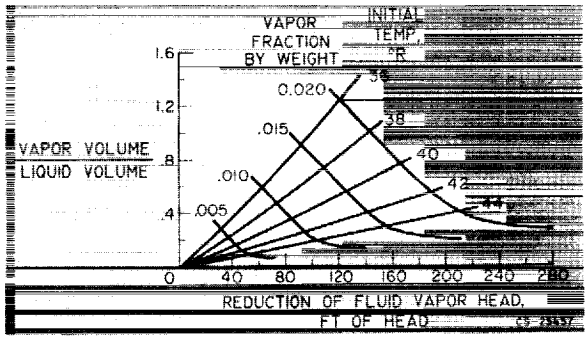

FIGURE 38–9.—Reduction of fluid vapor head due to hydrogen thermodynamic properties.

A thermodynamic chart that illustrates the basis for the difference in cavitation performance between liquid hydrogen and water is shown in figure 38–9. This theoretical plot shows the thermodynamic changes that occur when evaporation of part of the fluid reduces the vapor pressure and temperature of the liquid-vapor mixture. The ratio of vapor volume to liquid volume is plotted against the reduction in fluid vapor heat that occurs for evaporation from several initial liquid-hydrogen temperatures. Contours of the corresponding constant vapor weight fractions are also indicated. The interesting conclusion from this chart concerns the large reduction in fluid vapor pressure that can be achieved with a relatively small amount of evaporation. For example, if only 0.016 of the weight fraction of a quantity of hydrogen adjacent to the low-pressure surface of the blade were evaporated from an initial temperature of 36° R, equal volumes of liquid and vapor would result in the local region, and the local vapor pressure would be reduced about 100 feet below that of the fluid generally. This local reduction in vapor head corresponds approximately to the low-pressure curve shown in figure 38–8, the average of which corresponds approximately to the value of TSH. This analytical approach appears to be at least qualitatively useful in explaining the phenomenon. The required vaporization can occur locally in the region where vapor head reduction is specifically needed without subjecting the entire flow passage to a large volume of vapor. The amount of TSH achieved from this process depends on how effectively the various factors are utilized on the pressure loading diagram of a given pump blade design.

Better understanding of the hydrodynamic principles and the internal flow conditions during cavitation is necessary. Further research to determine definitive values of the hydrodynamic and thermodynamic interactions during cavitation will allow the designer to take full advantage of these principles.

HIGH-PRESSURE PUMP STABILITY

The problem of pump flow stability will be approached by noting the effects illustrated in figure 38–10. The variation in head rise with flow is shown in the upper left sketch of figure 38–10. At some low flow value the pump and system operated with violent pressure fluctuations and are said to have been stalled. Even in what appears to be a good region of flow, however, the pump head rise varied with time, as shown in the upper right sketch. The ratio of peak-to-peak variation in pressure head to the head rise in general $H_{p\text{-}p}/\Delta H$ varies with both the flow rate and the suction head above vapor pressure in the manner indicated by the lower sketches in figure 38–10. These pressure fluctuations are a result of unsteady flow configurations such as flow eddies. If the flow eddy exists near the pump discharge, and thus affects energy addition, the variation with Q can be expected to be a major factor. On the other hand, if the eddy condition exists near the inlet and can interact with cavitation, the variation shown with inlet head above vapor pressure can be expected to be large.

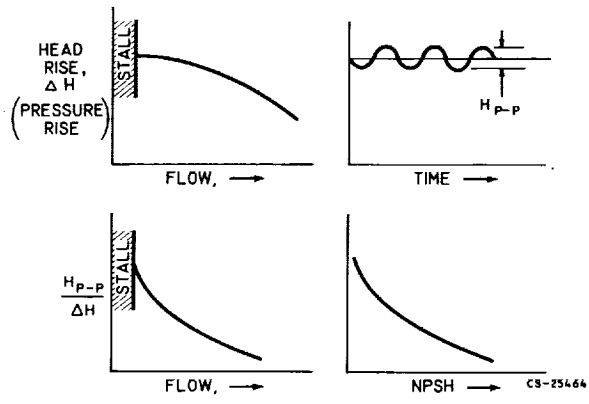

FIGURE 38–10.—Pump discharge pressure fluctuations due to unsteady flow conditions.

Before discussing the internal flow conditions which may affect pump stability, it would be well to describe the overall characteristics of hydrogen pumps. The pump shown in figure 38–11 is a research hydrogen pump rotor under investigation at the Lewis Research Center. When operated at 40,000 rpm (tip speed of about 1100 ft./sec) the power required to drive this rotor is of the order of 6000 horsepower. The pressure rise from inlet to outlet

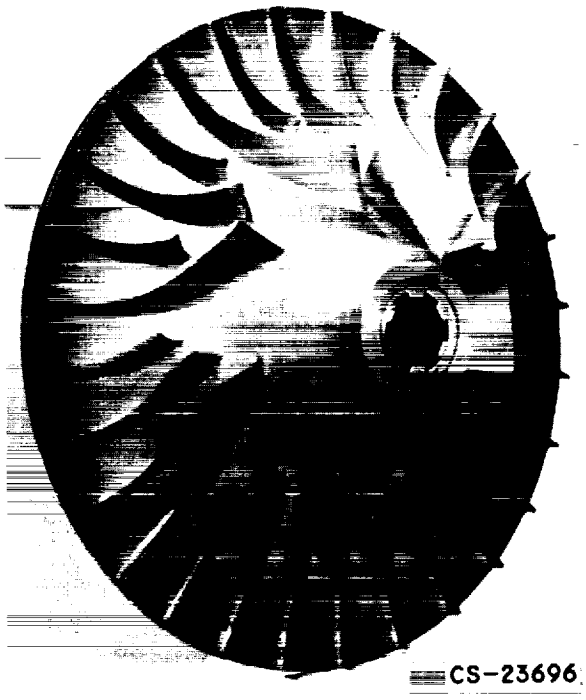

FIGURE 38–11.—Large flow hydrogen pump rotor.

under the conditions described is about 1000 pounds per square inch. High pressure and velocity gradients within the pump rotor are necessary to achieve this large transfer of energy from the rotor to the pumped fluid. The following discussion will consider the effects of excessive flow gradients within the pump rotor, and some of the methods of avoiding excessive flow gradients will also be indicated.

The velocity distribution between blades on a pump rotor is illustrated by the sketches in figure 38–12. The blades are presumed to be rotating to the right so that the high- and low-

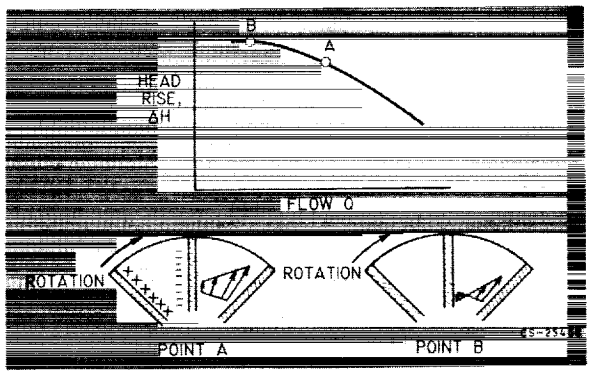

FIGURE 38–12.—Effect of passage pressure and velocity distribution on pump performance.

pressure surfaces of the blade are as indicated in the figure. A mean flow velocity exists near the passage center, a high velocity is associated with the low-pressure surface, and a low velocity is associated with the high-pressure blade surface. Such a velocity variation is necessary to achieve the energy transfer to the pumped fluid. At a slightly reduced flow, however, or in another design in which the mean velocity is reduced but a similar velocity distribution from blade to blade is required, the low-velocity flow may be reduced to zero or reversed flow may occur. The sketch on the right in figure 38–10 indicates a case in which reverse flow occurs over a portion of the passage. Such regions of reverse flow result in the formation of a flow eddy as illustrated by the flow streamlines shown in figure 38–13 (left sketch). If the flow eddies are of sufficient size, they may become unsteady. This unsteadiness may result from pressure fluctuations originating in the system external to the pump or those associated with the rotor blades passing the volute tongue. In this manner the small pressure fluctuations

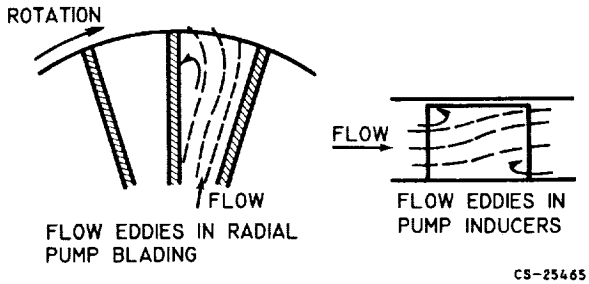

FIGURE 38–13.—Aspects of unsteady flow in pump rotors.

in the system may become amplified as a result of unsteady eddy flow conditions within the pump.

The right sketch in figure 38–13 shows a flow eddy that can occur in an inducer or axial-flow pump stage. The flow distribution at the rotor discharge must be such that, with the radial distribution of energy addition and flow losses, simple radial equilibrium exists. This usually requires that there be a radial outward shift of mass flow as the inducer is operated at reduced flow rates. The result is the formation of a flow eddy as shown at the discharge of the rotor hub. The accompanying streamline curvature can result in a simultaneous flow eddy near the rotor tip at the inlet. This type of flow eddy can also be involved in causing pressure fluctuations in a pump rotor similar to those described previously. Flow eddies can be avoided in design if additional blades are added to reduce the blade-to-blade velocity variation indicated in the left sketch of figure 38–13 or if the through flow velocity is increased to avoid zero flow velocities. In the case of the axial-flow configuration it may be necessary to reduce the overall loading to avoid premature flow eddies. The design restrictions resulting from these considerations may reduce the potential overall pump performance or efficiency but may be the compromises necessary to obtain stable operation over the desired flow range.

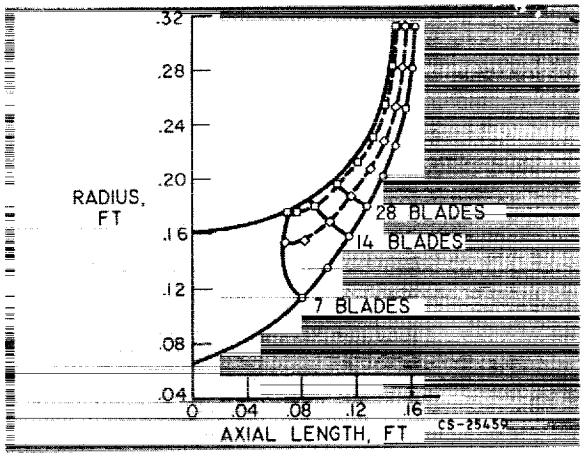

(a) Flow streamlines in plane of axis.

FIGURE 38–14.—Impeller velocity gradients calculated by stream-filament solution.

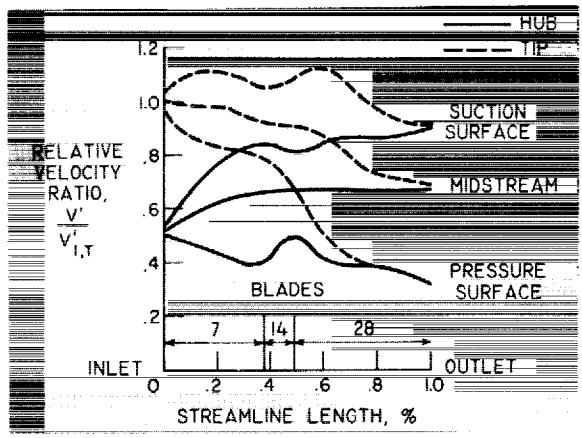

(b) Blade-to-blade solution.

FIGURE 38–14 (Concluded).—Impeller velocity gradients calculated by stream-filament solution.

One of the approximate theoretical methods of determining velocity distributions within an impeller is the stream-filament method. This method was utilized in the design of the pump rotor shown in figure 38–11. The calculated streamline flow and the velocity distribution on the blades are shown in figure 38–14(a). The streamlines are calculated in the axial plane by the previously mentioned stream filament solution. This assumes that the flow is at the blade angle and is symmetrical in the axial plane. It is assumed that the pressure varies linearly from blade to blade about the mean of the passage. By this approximation, which has been shown to be reasonably good for many cases, the blade surface velocities are calculated as shown in figure 38–14(b). The mean velocity at the rotor tip is shown to decrease slightly. The high- and low-velocity surfaces of the blade are displayed above and below the mean passage velocity. The rotor hub velocity is somewhat lower than the tip velocity. The low blade surface velocity along the hub can be kept from becoming zero by the addition of splitter vanes at several stations through the impeller. A mathematical relation between eddy size and flow stability is not as yet available except that it is known that pumps which experimentally exhibit large pressure fluctuations also indicate extensive eddy regions when this type of solution is used to calculate internal velocity distributions.

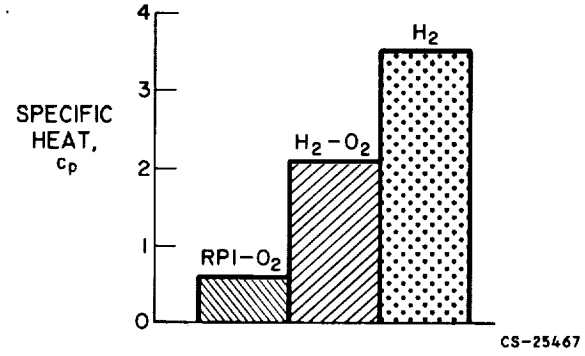

FIGURE 38–15.—Specific-heat comparison for turbine drive gases.

TURBINES FOR HIGH ENERGY

Hydrogen pumps require high power levels to move the liquid to the high-pressure engine. This results because a low-density fluid such as liquid hydrogen requires pumps of very high head rise (for a given pressure rise) and power is proportional to head rise. Compensating for this is the fact that hydrogen-rich gases have a very high heat content. This is illustrated in figure 38–15, where the specific heat of RPI (kerosene) oxygen, hydrogen-oxygen, and pure hydrogen gas are compared. The H_2–O_2 contains 3½ times the thermal energy of RPI–O_2 and the H_2 contains about six times the thermal energy of RPI–O_2. The problem becomes one of obtaining turbine geometry that extracts these high specific energies at reasonable turbine efficiency.

Turbine efficiency is shown in figure 38–16 plotted against the turbine speed-work parameter. A decrease in this speed-work parameter occurs as more energy is extracted from a given mass of working fluid passing through the turbine. Thus, as shown by figure 38–15, a single-stage turbine experiences a decrease in efficiency as more specific energy of the working fluid is extracted. An approximate region of performance of a turbine for hydrogen-oxygen gas is indicated as well as the anticipated performance of a hydrogen gas turbine. The turbine performance curves for different numbers of stages are anticipated as a result of reducing the work extracted in each stage. The contours for the various propellants are only meant to indicate that, if reasonable turbine efficiencies are to be obtained, it is necessary to use a considerable number of turbine stages for the high-energy propellants.

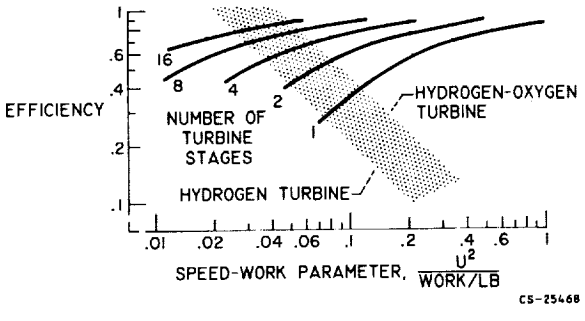

FIGURE 38–16.—Turbine-efficiency considerations for high-energy propellants.

In practice the achievement of the performance levels indicated in figure 38–14 requires the use of a sophisticated aerodynamic as well as mechanical design. Both the stators and the rotors must utilize a three-dimensional design technique similar to that described in the previous sections. The blade-surface diffusion must be controlled to suitable limits. The previous discussion shows that the turbine requirements cannot be met with a simple unsophisticated design.

The need for multistage turbines also results in increased mechanical problems. For example, large thrust unbalances can be encountered that must be handled by thrust bearings or balance pistons. Critical speeds of the running gear may occur in the region of design speed as a result of the larger rotating masses. The pressure drop over these multistage turbines may be very large and thus be accompanied by a very large expansion in flow area or blade height through the turbine. The value of obtaining high turbine efficiency is emphasized by the fact that the propellant bleed rate for turbine drive is inversely proportional to turbine efficiency. Since the drive fluid must be hydrogen-rich to hold the temperature to levels that the rotating parts can tolerate and the turbine exhaust is low in propulsive energy, a low turbine efficiency will result in a large increase in hydrogen tank size and a decided decrease in overall specific impulse. Because of the low density of hydrogen, the tankage and

system are large and heavy. Each pound of hydrogen carried into space must be utilized to its fullest extent.

SUMMARY OF DISCUSSION

The following summarizes the material presented on problem areas of turbomachinery:

1. Three areas were discussed as typical of the high level of design sophistication required in modern turbomachinery. These areas were

   a. The effect of cavitation on blade loading distributions

   b. The relation of pump pressure fluctuations to flow stability within the pump

   c. The desirability and complexity of multistage turbines

2. The discussion pointed out the necessity for extensive design efforts with particular efforts to understand the internal flow processes involved. This has become necessary because:

   a. In a rocket engine system the turbomachinery must be closely integrated with the other components. Turbopump efficiency affects propellant tank size and specific impulse, suction performance affects tank pressurization requirements and weight, and unstable operation could cause instabilities in many other components of the system.

   b. The development of a rocket engine is a stepwise process. Thus, if the turbopump does not perform as anticipated, extensive system changes may be necessary.

   c. In general, changes in the turbopump can result in extensive space program delays. In order to avoid such delays, it is often necessary to limit the changes, and this results in performance and/or reliability sacrifices.

3. Pumping machinery for our modern rocket engines cannot be considered an "off the shelf item." Because of the interrelation between turbopump characteristics and those of the engine system, it is necessary to design a turbopump for a given engine system rather than adapt an existing unit.

BIBLIOGRAPHY

Design of Cavitating Pump Inducers

MONTGOMERY, JOHN C.: Analytical Performance Characteristics and Outlet Flow Conditions of Constant and Variable Lead Helical Inducers for Cryogenic Pumps. NASA TN D–583, 1961.

ROSS, C. C., and BANERIAN, GORDON: Some aspects of High-Suction Specific-Speed Pump Inducers. Trans. ASME, vol. 78, no. 8, Nov. 1956, pp. 1715–1721.

SANDERCOCK, DONALD M., SOLTIS, RICHARD F., and ANDERSON, DOUGLAS A.: Cavitation and Noncavitation Performance of an 80.6° Flat-Plate Helical Inducer at Three Rotational Speeds. NASA TN D–1439, 1962.

STRIPLING, L. B.: Cavitation on Turbopumps, pt. 2. Paper 61–WA–98, ASME, 1961.

STRIPLING, L. B., and ACOSTA, A. J.: Cavitation in Turbopumps, pt. 1. Paper 61–WA–62, ASME, 1961.

Fluid Effects on Cavitation

HOLLANDER, A.: Theromdynamic Aspects of Cavitation in Centrifugal Pumps. ARS Jour., vol. 32, no. 10, Oct. 1962, pp. 1594–1595.

JACOBS, R. B., MARTIN, D. B., VAN WYLEN, G. J., and BIMMINGHAM, B. W.: Pumping Cryogenic Liquids. NBS Rep. 3569.

SALEMAN, VICTOR: Cavitation and NPSH Requirements of Various Liquids. Trans. ASME, ser. D, Jour. Basic Eng., vol. 81, 1959, p. 167.

STAHL, H. A., and STEPANOFF, A. J.: Thermodynamic Aspects of Cavitation in Centrifugal Pumps. Trans. ASME, vol. 78, 1956, p. 1691.

WILCOX, WARD W., MENG, PHILLIP R., and DAVIS, ROGER L.: Performance of an Inducer-Impeller Combination at or Near Boiling Conditions for Liquid Hydrogen. Paper presented at Cryogenic Eng. Conf., Los Angeles (Calif.), Aug. 14–16, 1962.

Pump Internal Flow Design Consideration

HAMRICK, JOSEPH T., GINSBURG, AMBROSE, and OSBORN, WALTER M.: Method of Analysis for Compressible Flow through Mixed-Flow Centrifugal Impellers of Arbitrary Design. NACA Rep. 1082, 1952. (Supersedes NACA TN 2165).

OSBORN, WALTER M., SMITH, KENNETH J., and HAMRICK, JOSEPH T.: Design and Test of Mixed-Flow Impellers. VIII—Comparison of Experimental Results for Three Impellers with Shroud Redesigned by Rapid Approximate Method. NACA RM E56L07, 1957.

SMITH, KENNETH J., and HAMRICK, JOSEPH T.: A Rapid Approximate Method for the Design of Hub Shroud Profiles of Centrifugal Impellers of Given Blade Shape. NACA TN 3399, 1955.

WU, CHUNG-HUA: A General Theory of Three-Dimensional Flow in Subsonic and Supersonic Turbo-machines of Axial-, Radial-, and Mixed-Flow Types. NACA TN 2604, 1952.

Turbine Design Considerations

GINSBURG, AMBROSE, HARTMANN, MELVIN, and STEWART, WARNER: Review of Problems Encountered in Turbomachinery Design for Advanced Propulsion Systems. Paper 62–AV–23, ASME, 1962.

STEWART, W. L.: A Study of Axial-Flow Turbine Efficiency Characteristics in Terms of Velocity Diagram Parameters. Paper 61–WA–37, ASME, 1961.

STEWART, WARNER L.: Analytical Investigation of Multistage-Turbine Efficiency Characteristics in Terms of Work and Speed Requirements. NACA RM E57K22b, 1958.

Text Books

SHEPARD, D. G.: Principles of Turbomachinery. The MacMillan Co., 1956.

SPANNHAKE, WILHELM: Centrifugal Pumps, Turbines, and Propellers. The Technology Press, M.I.T., 1934.

STEPANOFF, A. J.: Centrifugal and Axial-Flow Pumps. Second ed., John Wiley & Sons, Inc., 1957.

VAVRA, M. H.: Aero-Thermodynamics and Flow in Turbomachines. John Wiley & Sons, Inc., 1960.

WISLICENUS, G. F.: Fluid Mechanics of Turbomachinery. McGraw-Hill Book Co., Inc., 1947.

39. Recent Aspects of Rocket Combustion Research

By Gerald Morrell and Richard J. Priem

GERALD MORRELL, *Chief of the Chemical Rocket Fundamentals Branch at the Lewis Research Center, has specialized in the fields of heat transfer, combustion, hydrodynamics, gas dynamics, and chemistry. He earned his B.S. degree in Chemical Engineering from Wayne State University in 1943, and his M.S. degree in Chemical Engineering from the University of Michigan in 1948. Mr. Morrell is a Senior Member of the American Rocket Society, an Associate Fellow of the Institute of Aerospace Sciences, a Member of the American Institute of Chemical Engineers, and a licensed professional engineer of the State of Ohio. He received the Rockefeller Public Service Award in 1957.*

DR. RICHARD J. PRIEM, *Head of the Rocket Combustion Section at the NASA Lewis Research Center, is currently working in research on combustion and fluid flow studies. A native of Mayville, Wisconsin, Dr. Priem attended the University of Wisconsin, where he earned his B.S., M.S., and Ph. D. degrees.*

In the broadest sense, all forms of combustion are similar because they involve the reaction of a reducing agent (fuel) and an oxidizing agent to produce reaction products with the liberation of heat. Such a broad concept can be useful in bringing together the results of diverse researches, but is of little value in guiding a particular program of research, because the boundary conditions determine the rate-limiting steps. It is these boundary conditions that guide the research worker in the selection of theoretical and experimental approaches to the goal of understanding or, at least, characterization. The specialization of combustion research or research, in general, arises when attention is confined to a particular set of boundary conditions.

If the case of a combustion wave propagating through initially premixed gases, or the equivalent, a stabilized wave in a flowing system is considered, the problem is in the realm of classical flame studies that have occupied the attention of researchers for many decades. The results of these studies are basic to all other areas of combustion research, since in this case it is the chemistry that is rate limiting. Consider next a different boundary condition of initially unmixed gases. This produces a diffusion flame in which the overall conversion rate is governed by mixing rather than by chemical kinetics. A still more complicated set of boundary conditions is provided by initially unmixed liquid or solid reactants. Rocket-combustion research is concerned with problems arising out of this set of conditions. In addition to flame chemistry and gas phase mixing, other processes should be considered such as phase transitions, heat and mass transfer between phases, hydrodynamics of atomization, liquid mixing, viscoelastic behavior, and condensed phase reactions. There are, of course, many ways of approaching a complicated set of competing and sequential processes. At the NASA Lewis Research Center, two complementary approaches are being followed. (1) An attempt is made to devise simplified conceptual models of the combustion system that can give quantitative predictions of system behavior from the conservation equations; the predictions then must be checked experimentally. (2) Individual rate processes are

studied with the hope that increased knowledge will enable generation of more realistic models. Of course, this kind of research also stands by itself, since the results, ideally, represent a net gain in the understanding of a variety of physical and chemical processes.

For this presentation, one example of each approach to learning is discussed in detail. The first example is concerned with the interesting phenomenon of combustion resonance and, in particular, with the question of the magnitude of disturbance that leads to instability or resonance burning.

Under certain conditions that are not yet well understood, one or more acoustic modes of the combustor may be excited to large amplitudes. For combustors with large length-to-diameter ratios, the axial mode is usually observed, while for small length-to-diameter ratios the transverse or spinning transverse modes are more apt to occur. These waves interact with the combustion processes to produce large variations in the local heat-release rates. From a practical standpoint, the results are often deleterious: increased heat flux rates can cause wall failures and the vibration may induce structural failures. The transverse modes are especially severe with respect to the first type of failure.

Another common mode of instability is that produced by the coupling of combustor pressure variations with those in the feed system. The characteristic time for these oscillations is determined by the filling time of the combustor. This form of instability will be discussed in the paper by J. C. Sanders.

The geometric model chosen for analysis of the transverse mode is shown in figure 39–1.

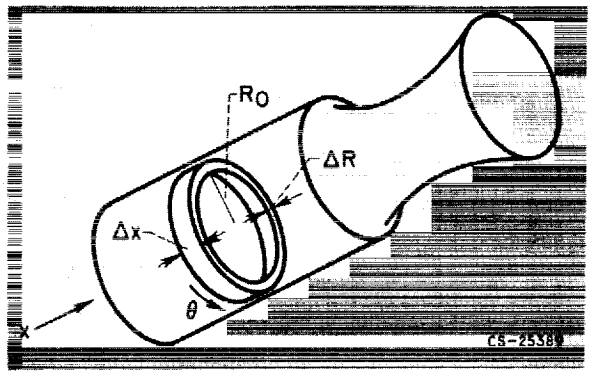

FIGURE 39–1.—Model used for instability analysis.

An annular section of a cylindrical combuster is imagined, a pressure or velocity disturbance of finite magnitude is introduced at one location, and the growth (or decay) of the wave is computed as it travels along the annulus. Simultaneous solutions of the conservation equations and an expression for the burning rate are required. The equation for conservation of momentum is

$$\frac{\partial}{\partial t}(\vec{\rho v}) = -\vec{\nabla}\cdot(\vec{\rho v}\cdot\vec{v}) - g\vec{\nabla}P - \vec{\nabla}:\tau + \vec{W v_l}$$

According to this equation the accumulation of momentum is the sum of the convective flow term, the viscous dissipation term, and the mass addition term. In nondimensional form the equation becomes

$$\frac{\partial}{\partial t^*}\left(\frac{P^*}{T^*}\vec{v^*}\right) = -\vec{\nabla}^*\cdot\left(\frac{P^*}{T^*}\vec{v^*}\cdot\vec{v^*}\right) - \left[\left|\frac{1}{\gamma}\right|\right]\vec{\nabla}^*P^* - \left[\left|\frac{\mu_0}{R\rho_0 V_0}\right|\right]\vec{\nabla}^*:\vec{\tau}^* + \left[\left|\frac{Rw_0}{\rho_0 V_0}\right|\right] w^*\vec{v_l^*}$$

where ρ is gas density, $\vec{v}$ is gas velocity, v_l is liquid velocity, w is the local instantaneous burning rate, P is pressure, V_0 is velocity of sound, R is radius, μ is velocity, and the subscript 0 refers to steady-state conditions. The second parameter on the right side is a Reynolds number based on the velocity of sound, and the third parameter is analogous to Damkohlers first similarity group.

The equation for average burning rate is

$$m = \left[\frac{1+\left(\frac{w_0}{w_f}\right)_{ST.}}{1+\left(\frac{w_0}{w_f}\right)}\right] \frac{\mathscr{K}(P_0/300)^{0.5}}{\mathscr{A}^{0.3}(1-T_r)^{0.2}\left(\frac{\varkappa_m}{0.003}\right)^{1.5}\left(\frac{V_j}{1200}\right)^{0.8}}$$

where w_o and w_f are oxidant and fuel flow rates, respectively, T_r is reduced liquid temperature, $\mathscr{A}$ is the ratio of combustor cross-sectional area to nozzle cross-sectional area (A_c/A_t), $\varkappa_m$ is mass-medium drop size, V_j is injection velocity, and $\mathscr{K}$ is a constant that depends on liquid properties. This equation is applicable to steady-state vaporization, and its use here indicates two of the

major assumptions in the development: (1) vaporization is the rate-controlling process, and (2) the response of the process to a disturbance is quasi-steady state. The second assumption is especially serious, but in the absence of data on the time variation of vaporization it is the best that can be done now.

The parameters mentioned in connection with the nondimensional momentum equation are converted to rocket nomenclature as follows:

Burning Parameter:

$$\frac{Rw_0}{\rho_0 V_0}=\frac{Rm}{\mathscr{A}}\sqrt{\left(\frac{2}{\gamma-1}\right)^{\frac{\gamma+1}{\gamma-1}}}$$

$$\mathscr{L}\equiv\frac{Rm}{\mathscr{A}}$$

Dissipation Parameter:

$$\frac{\mu_0}{\rho_0 R V_0}=\frac{\mu_0 c^*}{RP_0 g}\sqrt{\left(\frac{2}{\gamma-1}\right)^{\frac{\gamma+1}{\gamma-1}}}$$

$$\mathscr{J}\equiv\frac{\mu_0 c^*}{RP_0 g}$$

where m is the fractional liquid consumption per unit length; and c^* is characteristic velocity $P_0 A_t g/\dot{W}$ where $\dot{W}$ is total mass flow rate. The $\mathscr{L}$ term represents the steady-state intensity of combustion, while the $\mathscr{J}$ term represents the viscous damping. The general stability diagram that results from the solution of the equations is shown in figure 39–2, where nondimensional wave amplitude is plotted as a function of the $\mathscr{L}$ factor for several values of the relative gas velocity with respect to the liquid phase. Here Δv is $\frac{|\vec{v}-\vec{v}_l|}{V_0}$. The $\mathscr{J}$ factor does not appear, because for the one-dimensional case considered boundary-layer effects and other damping processes are negligible. The lower curves in the figure represent the threshold values of disturbance amplitude that will result in wave amplification; the upper band represents the equilibrium amplitude of the wave. Several interesting points are immediately apparent. No matter what flow conditions are imposed, there is always a minimum in the threshold amplitude that increases with an increase in relative velocity (Δv). This

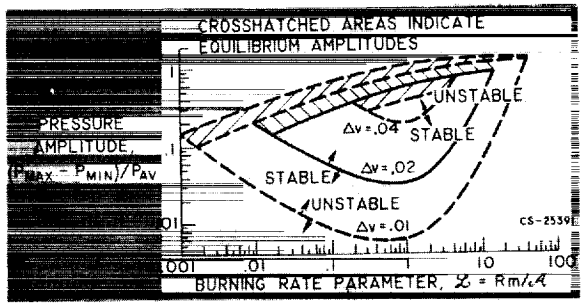

FIGURE 39–2.—Stability plot for vaporization model with various velocity differences.

implies that low contraction ratio combustors would be most stable providing that some way were available to keep the liquid phase from accelerating to gas velocity. The minimums, which occur in a small range of $\mathscr{L}$ values, indicate a region of space-heating rates that should be avoided for maximum stability. The most interesting feature is that the theory predicts absolute stability at sufficiently high heating rates. Qualitatively, this means that if the axial momentum becomes sufficiently large, all disturbances will be damped. Currently an experiment is being initiated to check this conclusion. A toroidal combustor several feet in diameter will be employed, which has been designed to obtain values of $\mathscr{L}$ well into the stable region. In the absence of definitive data, however, it might be useful to examine qualitatively the relation between $\mathscr{J}$ and $\mathscr{L}$ for available reactor data. Such a relation is shown in figure 39–3, where vaporization has been assumed to control the burning process.

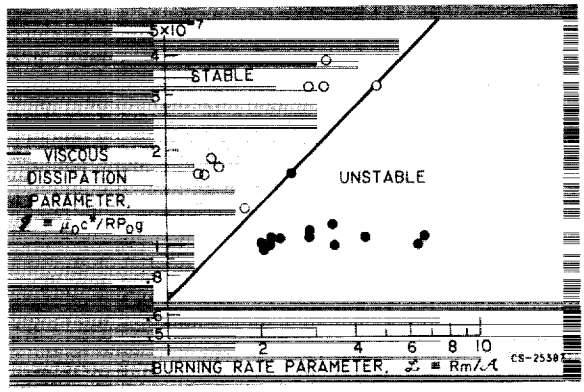

FIGURE 39–3.—Stability plot based on fuel-jet breakup by a shock wave.

It is possible to obtain a clear separation of stable and unstable combustors. If the theory is correct, there should be a second stable region for values of $\mathscr{L}$ much larger than those shown in the figure. This empirical plot indicates that the assumption of a single slow rate process may be valid for describing the stability of a complex system.

The second example of research is concerned with measuring the rate of atomization of a liquid jet by a transverse shock wave. Interest in this question stems from the elementary notion that, in vaporization-limited combustion, a velocity disturbance or steady-state wave that produced a rapid increase in liquid surface area could be amplified and driven.

To simplify matters, study of the phenomenon has been made in the absence of combustion and in a shock wave rather than an oscillating flow. A schematic diagram of the experimental arrangement is shown in figure 39–4. A variable-length high-pressure section provides gas flows of varying duration, and the atomization is recorded by both frame and streak photographs. Examples of the data are shown in figure 39–5. It appears that at least two modes of breakup occur: (1) a deformation into sheets of liquid, and (2) atomization by streaming from the liquid surface. The theoretical model chosen for examination is a boundary layer on a flat plate of liquid as an approximation of the streaming phenomenon. The rate of atomization is then given by the product of boundary-

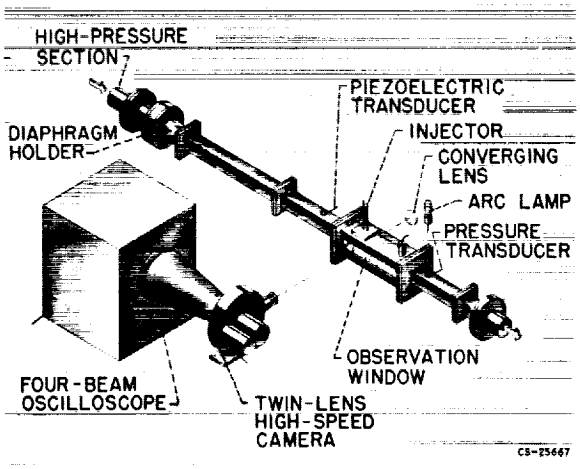

FIGURE 39–4.—Schematic diagram of experimental arrangement.

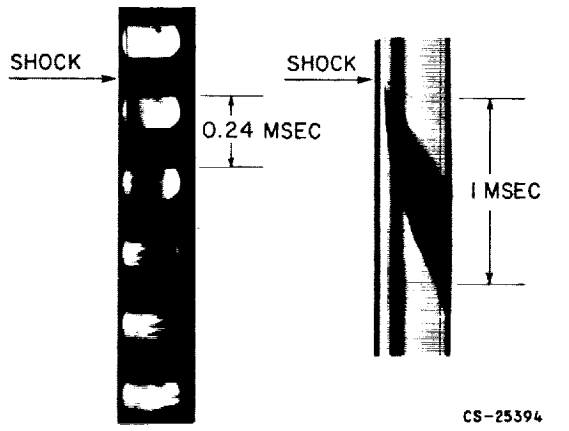

FIGURE 39–5.—Examples of photographic data of jet breakup. Shock velocity, 1655±5 feet per second; gas velocity, 732±5 feet per second; jet diameter, 0.052 inch.

layer thickness and velocity evaluated at the rear edge of the sheet. On the basis that surface tension determines the stable length of a liquid sheet, it can be shown that the length should be a function of Weber number and the square root of Reynolds number. The actual expression for maximum length (derived from streak pictures) is

$$\frac{L}{2R_0}=1+2\frac{We_0}{\sqrt{Re_0}}$$

where R_0 is the initial radius of the jet; We_0 is the Weber number $R_0u^2\rho/\sigma$ where u is the gas velocity behind the shock wave relative to the liquid, ρ is gas density, and σ is interfacial tension; and Re_0 is the Reynolds number $R_0u\rho/\mu$ where μ is gas viscosity. This linear relation is the simplest one that describes the data. The boundary-layer thickness and velocity were determined by solving von Kármán's momentum equations with a modified Sanborn-Kline laminar velocity profile for both the gas and liquid phases. The final equation is

$$t_b=0.536\left(\frac{\rho_l}{\rho_g}\right)^{2/3}\left(\frac{\mu_g}{\mu_l}\right)^{1/3}\frac{R_0}{u}\sqrt{\frac{Re_0}{1+2\dfrac{We_0}{\sqrt{Re_0}}}}$$

where t_b is the time for complete atomization and the other terms have their usual significance with the subscripts g for the gas phase and l for

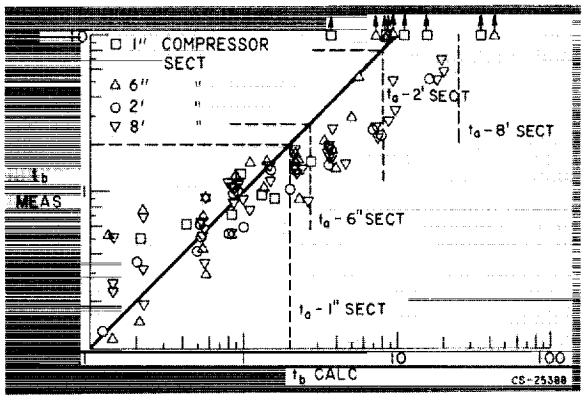

FIGURE 39–6.—Comparison of experimental and calculated atomization times based on boundary-layer theory.

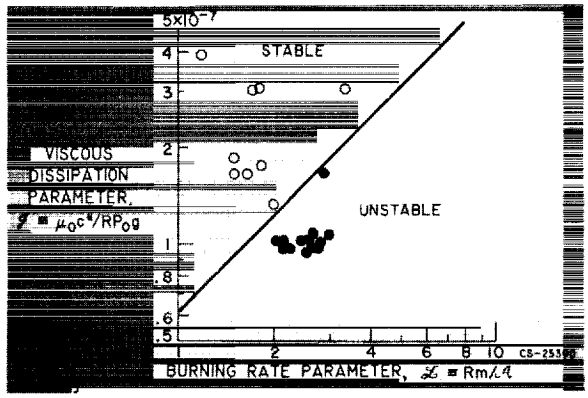

FIGURE 39–7.—Stability plot based on steady-state propellant vaporization.

the liquid phase. In figure 39–6, the measured values of breakup time are compared with the calculated values. The arrows indicate incomplete breakup, and the dashed boundaries are the limits of gas flow duration for the corresponding length of high-pressure section. Although the agreement is far from perfect, the model appears to be basically correct. Experiments with other fluids are required to test the theory adequately and certainly the effects of ambient pressure and combustion need to be evaluated. Some of these experiments are now being conducted. Figure 39–7 shows a plot similar to the one in figure 39–3 but with the fractional burning rate evaluated in terms of jet atomization. Such an empirical plot hardly represents a test of the theory, but it does show again that a single rate-limiting process may be used to describe the response of a combustion system to a disturbance.

Much more research is needed on the processes of rocket combustion, not only to satisfy scientific curiosity but also to make a contribution to the need for ever-increasing reliability. Experimental and theoretical work on more realistic system models would certainly be desirable. The physics and chemistry of many other rate processes need thorough investigation, especially the response of the processes to a disturbance. At low combustion pressures, chemical kinetics might be expected to become the dominant factor, while at very high pressures the unburned phase may become supercritical, and turbulent mixing could be an important process. For fuels and oxidants that react on contact, interfacial liquid-phase-reaction kinetics may be important. Consideration of initially solid reactants involves the study of gas-solid reactions. These considerations are only illustrative of the many challenges awaiting the researcher in combustion theory and practice.

BIBLIOGRAPHY

The following references are pertinent to the present discussion:

MORRELL, G.: Critical Conditions for Drop and Jet Shattering. NASA TN D–677, 1961.

MORRELL, GERALD: Breakup of Liquid Jets by Transverse Shocks. Eighth Symposium (International) on Combustion, The Williams & Wilkins Co., 1962, pp. 1059–1068.

PRIEM, R. J., and MORRELL, G.: Application of Similarity Parameters for Correlating High Frequency Instability Behavior of Liquid Propellant Combustors. Progress in Astronautics and Rocketry. Vol. 6—Detonation and Two-Phase Flow, Academic Press, 1962, pp. 305–320.

PRIEM, RICHARD J., and GUENTERT, DONALD C.: Combustion Instability Limits Determined by a Nonlinear Theory and a One-Dimensional Model. NASA TN D–1409, 1962.

PRIEM, RICHARD J., and HEIDMANN, MARCUS F.: Propellant Vaporization as a Design Criterion for Rocket-Engine Combustion Chambers. NASA TR R–67, 1960.

For alternative approaches to the study of unstable combustion the following references are recommended:

CROCCO, L., and CHENG, S. I.: Theory of Combustion Instability in Liquid Propellant Rocket Motors. AGARD Monograph 8, Butterworths Sci. Pub. (London), 1956.

CROCCO, L., HARRJE, D. T., and REARDON, F. H.: Transverse Combustion Instability in Liquid Propellant Rocket Motors. Jour. Am. Rocket Soc., vol. 32, no. 3, Mar. 1962, pp. 366–373.

MCCLURE, F. T., HART, R. W., and BIRD, J. F.: Acoustic Resonance in Solid Propellant Rockets. Jour. App. Phys., vol. 31, no. 5, May 1960, pp. 884–896.

Recommended general references on combustion are:

LEWIS, B., and VON ELBE, G.: Combustion, Flames, and Explosions of Gases. Academic Press, Inc., 1951.

LEWIS, B., PEASE, R. N., and TAYLOR, H. S., eds.: Combustion Processes. Vol. II of High Speed Aerodynamics and Jet Prop., Princeton Univ. Press, 1956.

PENNER, S. S.: Chemistry Problems in Jet Propulsion. Pergamon Press, 1957.

PROPULSION CHEMISTRY DIVISION: Basic Considerations in the Combustion of Hydrocarbon Fuels with Air. NACA Rep. 1300, 1957.

SUBUGUE, J., ed.: Experimental Methods in Combustion Research, AGARD, Pergamon Press, 1961.

VON KÁRMÁN, T.: Fundamental Equations in Aerothermo-Chemistry. AGARD, Selected Combustion Problems, II. Butterworths Sci. Pub. (London), 1956.

40. Current Research and Development on Thrust Chambers

By Edmund R. Jonash and William A. Tomazic

EDMUND R. JONASH *is currently Chief of the Apollo Propulsion Office at the NASA Lewis Research Center. He has specialized in research of reciprocating engine fuels, turbojet engine fuels, turbojet engine combustion, and chemical rockets. A native of Kenton, Ohio, Mr. Jonash received a B.S. degree in Chemical Engineering from Massachusetts Institute of Technology in 1944. Mr. Jonash is a member of the American Rocket Society.*

WILLIAM A. TOMAZIC, *an Aerospace Scientist at the NASA Lewis Research Center, has specialized in the field of chemical rocket thrust chambers. A native of Cleveland, Ohio, Mr. Tomazic received his B.S. and M.S. degrees in Mechanical Engineering from Case Institute of Technology. He is a member of Tau Beta Pi and the American Rocket Society.*

INTRODUCTION

A million pounds of thrust for large boosters, a few ounces of thrust for attitude control systems—this is the range in size of thrust chambers that are under development today. Basic operating principles are the same for all sizes. The state of the art, however, is such that optimum thrust-chamber designs cannot be scaled from one size to another, and each new rocket engine procurement requires an extensive development program that is heavily dependent on cut-and-try experimental tests to meet system performance requirements.

The present state of the art of the chemical rocket thrust chamber, its principal problems and how they are being solved today are described herein. The areas of research and development that are required to provide the necessary improvements in system performance and operating characteristics to meet tomorrow's needs are indicated.

The thrust chamber illustrated in figure 40–1 is typical of a liquid-bipropellant rocket, in which the fuel and oxidizer are pumped into a propellant injector located at the forward end of the thrust chamber. The propellants are sprayed into the combustion chamber from many small orifices distributed over the face of the injector; they then vaporize, mix, ignite, and burn to produce high-temperature gases that are expanded through the nozzle to give thrust. This process occupies a total of some 3 to 4 milliseconds from injection of the propellants to ejection of the gases from the nozzle. Gas temperatures in the combustion zone vary

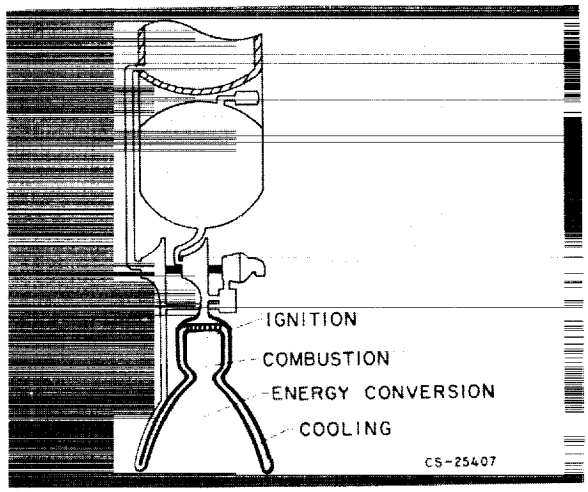

FIGURE 40–1.—Thrust chamber of chemical rocket.

666582 O—62——4

from 5000° to 8000° F depending upon the propellants used; pressures in current engines vary, with design, from 50 to 1000 pounds per square inch absolute.

The principal requirements of the thrust chamber are satisfactory ignition, stable and efficient combustion, maximum conversion of thermal to kinetic energy in the nozzle, and adequate cooling to maintain structural integrity of the chamber. These requirements are discussed in some detail. Some additional requirements are frequently involved but they are not discussed. These requirements include thrust vector control, which is necessary to provide control of vehicle direction and stability; hot-gas generation for supplying the turbopump drive turbine; and energy source for heating propellant-tank pressurizing gases.

IGNITION

Ignition in the chemical rocket must be reliable, reproducible, and rapid. Reliability is an obvious requirement. Reproducibility in terms of reaction time is particularly important in multiengine clusters in order that all engines start uniformly and no excessive thrust unbalances are produced. Ignition must be rapid to avoid accumulation of unburned propellants, which upon finally reacting will result in a high-pressure pulse. This pulse may be severe enough to rupture the chamber or trigger destructive combustion instabilities.

With hypergolic propellants, satisfactory ignition means providing for proper mixing of the propellants so that reaction may begin rapidly and smoothly. With nonhypergolic propellants, it means not only mixing the propellants, but also providing a separate energy source sufficient to initiate reaction. Various ignition energy sources have been used; some are illustrated in figure 40–2. Electrical-spark ignition systems have been used to produce ignition and, in fact, are used in restartable rocket systems that are currently under development. These systems are similar in principle to those used in reciprocating engines but must operate at a much higher energy level to assure satisfactory ignition. The principal problems inherent in such systems are assuring the presence of an inflammable mixture in the very localized area of energy release of a spark and providing adequate cooling of the spark plug during engine operation. A second method commonly used for rocket ignition is the injection of a chemical that is spontaneously inflammable with one of the two main propellants. The ignition propellant is introduced simultaneously with the appropriate main propellant. Reaction is initiated. The other main propellant is then injected and reacts, completing the ignition sequence. The ignition propellant may be injected separately into the combustion chamber, as illustrated in figure 40–2. Sometimes it has been introduced as a "slug" of liquid directly within one of the propellant feed systems; the slug is initially isolated from the propellants by frangible diaphragms. The third system shown in figure 40–2 is the pyrotechnic, which is simply a solid-propellant charge located near the injector. The solid propellant charge is ignited by an electric pulse. The resulting combustion provides the energy source for main-propellant ignition. For rocket systems requiring but one start, the pyrotechnic method has been favored because of its simplicity and reliability. The charge can be designed to provide a large excess of energy, and this energy can be distributed over a substantial volume of the chamber. A major problem encountered in use has been damage to the thrust-chamber walls by the burning solid charge. The scheme is not applicable to systems requiring multiple starts. Two additional ignition methods are catalysts and propellant additives. These methods are, as yet, only laboratory curiosities that require

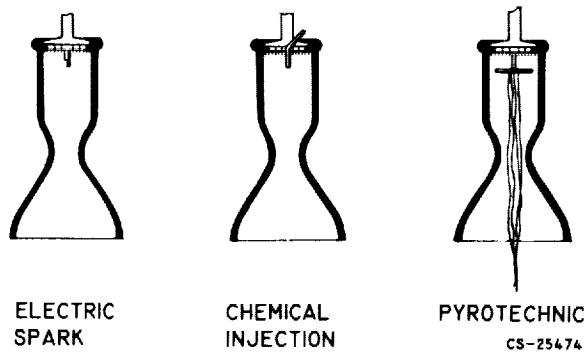

FIGURE 40–2.—Ignition techniques for nonhypergolic propellants.

much more research and development effort before they can be considered for application. Promising research has been conducted on ozone bifluoride (O_3F_2) as an additive for liquid oxygen to induce hypergolic ignition with hydrogen. Laboratory experiments have indicated that ozone bifluoride concentrations as low as 1 part in 2000 are sufficient to provide ignition. The nature of the reactions involved has not been determined, and the practical applicability of this technique has not yet been defined. Research in this area is continuing. Platinum has been considered as a potential catalyst for hydrogen-oxygen ignition. This area, although promising, has been little explored. Research into the nature of catalyzed reactions at very low temperatures (40° to 140° R) is required.

In general, ignition systems have been developed to a satisfactory level of reliability to meet the requirements of rocket systems now in use. There has not yet been enough experience, however, in deep-space propulsive flights to assure that these same systems are adequate for the more sophisticated missions now planned. Also, the introduction of the high-thrust engine intensifies the problem of igniting a large volume of propellant mixture in a controlled fashion that will assure establishing stable combustion conditions. The introduction of man into our rocket-propelled flights imposes greatly increased reliability requirements on critical components such as the ignition system. Additional effort is required to define better the potential capabilities of some of the more advanced systems that have been investigated. Passive systems such as additives and catalysts warrant particular attention in the laboratory since such systems have potentially higher reliabilities. Most of the effort must be concentrated on hydrogen-oxygen since a very large part of our space propulsion development is committed to this combination.

COMBUSTION EFFICIENCY

The potential space mileage from a chosen propellant combination is represented by its theoretical specific impulse. How well this potential is translated into actual performance is a function of two principal factors, combustion

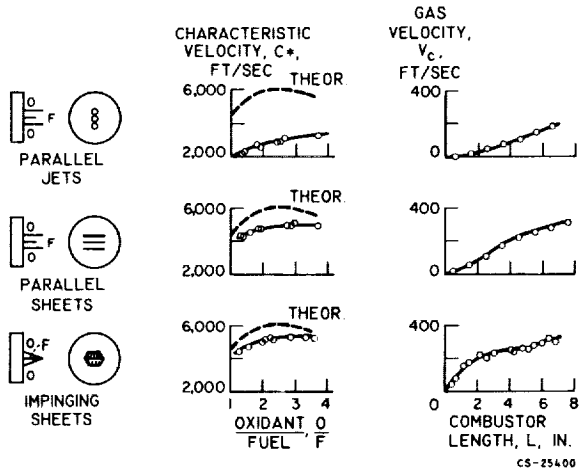

FIGURE 40-3.—Effect of injector element design on performance.

efficiency and exhaust-nozzle efficiency. Combustion efficiency is most dependent on the design of the propellant injector. A number of basic injector designs have been evolved during the course of development of our current engines; within these basic designs, thousands of variations in details are frequently tested before a satisfactory design is achieved. Some of these basic designs are illustrated in figure 40-3: (1) parallel jets that yield poorly atomized streams of propellant and do not promote cross mixing of the fuel and oxidant streams, (2) parallel sheets that are produced by pairs of fuel-on-fuel and oxidant-on-oxidant impinging jets and give improved atomization but still limited mixing, and (3) fuel-on-oxidant impinging jets that promote both mixing and atomization. The first set of curves shows the effect of injector design on the characteristic velocity, which is a measure of combustion efficiency. As might be expected, improvements in atomization and mixing reflect directly in improved performance, with experimental results ultimately approaching the theoretical maximum. The next set of curves of gas velocity and combustor length verify this improvement by showing that with improved atomization and mixing, combustion takes place more rapidly, that is, closer to the injector. These data were obtained with a liquid-oxygen–hydrocarbon propellant combination.

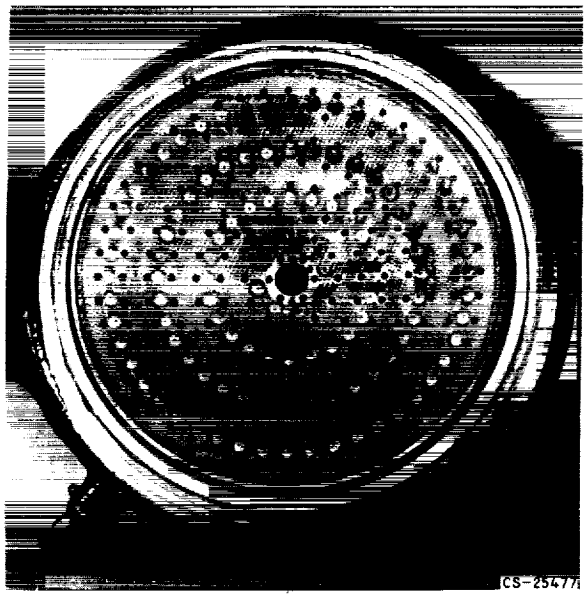

FIGURE 40–4.—Multielement 15,000-pound thrust injector.

In addition to its function in atomizing and mixing the propellants efficiently, the injector must provide a uniform distribution of mixture over the cross section of the chamber in order to make maximum use of the combustion space. Thus, injectors generally incorporate a large number of individual elements. As an example, figure 40–4 shows the face of an injector for a 15,000-pound thrust chamber; this injector contains 216 fuel and oxidant elements. If a 1,500,000-pound-thrust system were scaled up from this injector on a logical basis of constant thrust per element, 21,600 elements would be required. The fabrication of such injectors for a large rocket-engine development program would be extremely time consuming and expensive.

Two vital needs are evident: (1) quantitative criteria for injector design to reduce the number of injectors required to be investigated in a development program, and (2) simpler designs capable of higher thrust per element without sacrifice in performance. These needs will be even more critical in the development of propulsion systems that include a throttling capability, since such systems may utilize more complex, variable-geometry injection elements. The manned lunar landing is an outstanding example of a mission requiring this kind of increased operational flexibility.

COMBUSTION INSTABILITIES

If combustion efficiency were the only consideration, the choice of injector design would be reasonably straightforward; however, two other important requirements of the thrust chamber become involved: combustion stability and thrust-chamber durability. Experience indicates that thrust chambers with injectors providing high performance are frequently prone to combustion instabilities. The paper by Gerald Morrell and Richard J. Priem discussed fundamental studies of combustion instability. Some practical aspects of the problem are discussed briefly herein.

As has been noted, there are two principal kinds of instability, low-frequency "chugging" and high-frequency "screaming." Chugging is discussed in relation to control systems in the paper by John C. Sanders and Leon M. Wenzel. The most troublesome and least understood kind of combustion instability is the high-frequency screaming. The effect of such instabilities on thrust-chamber operation is illustrated in figure 40–5. Shown in figure 40–5(a) is a pressure trace typical of these oscillations. The frequency is inversely proportional to the chamber and in most applications is greater than 1000 cps. The predominant mode of damage is not a direct result of the pressure excursions, but rather it is a result of the scrubbing action of the oscillating gases causing very large increases in heat-transfer rate at the thrust-

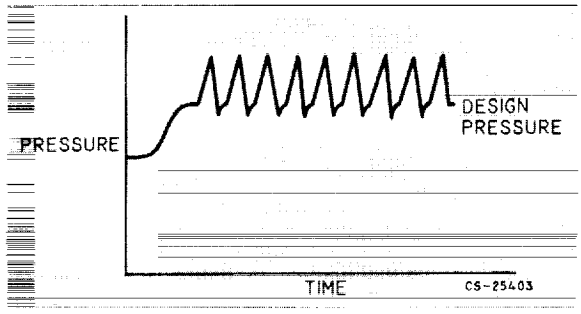

(a) Chamber pressures with screaming.

FIGURE 40–5.—High-frequency instability.

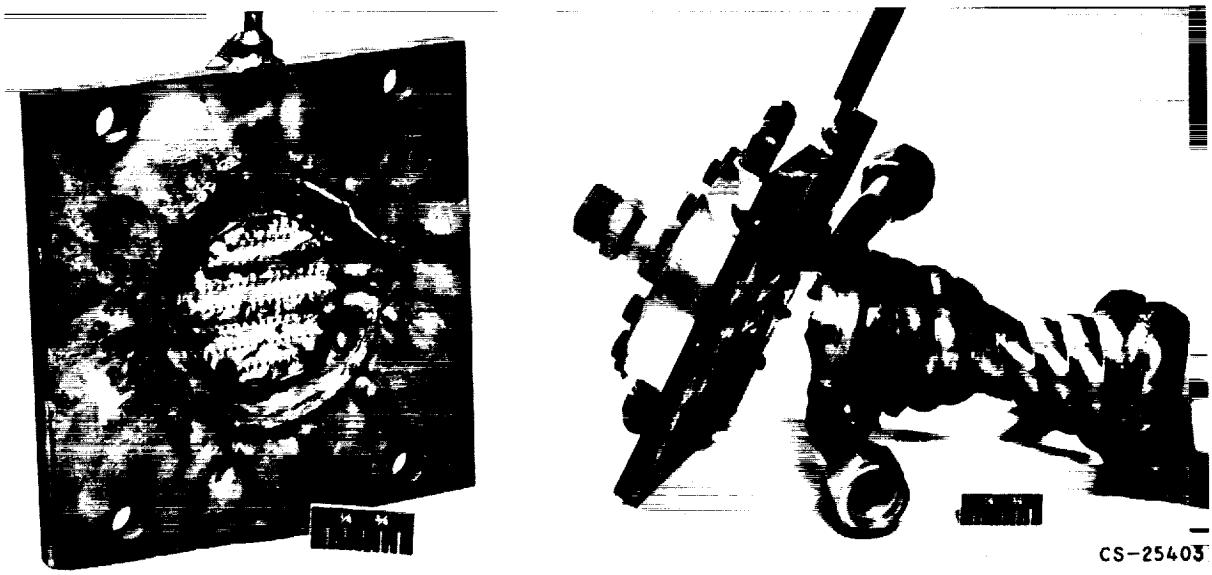

(b) Failure resulting from screaming.
FIGURE 40–5 (Concluded).—High-frequency instability.

chamber wall. A failure resulting from screaming in a laboratory thrust-chamber unit is shown in figure 40–5(b). The "burnout" occurred at the face of the injector, and the burn patterns indicated a rotary motion of the wave front. The severity of the heat-transfer increase is indicated by the fact that burnout occurred in approximately ½ second with a water-cooled chamber designed to provide a substantial cooling margin under stable combustion conditions.

One remedy for this mode of oscillation that has been widely investigated experimentally is the use of baffles on the face of the injector to compartment and break up the rotary motion. Figure 40–6 depicts an injector combining radial baffles and a circular, centrally located baffle. The radial baffles are intended to prevent tangential oscillations while the circular baffle is intended to prevent radial oscillations. The number of baffles, their design, and their dimensions are all parameters that thus far must be determined experimentally.

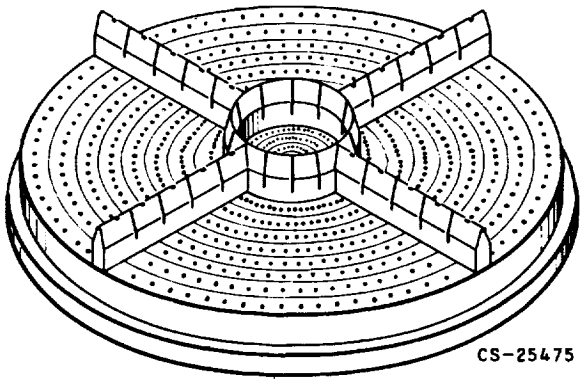

FIGURE 40–6.—Injector with baffles.

Other possible means of eliminating or alleviating destructive high-frequency oscillations include variations in injector element patterns and thrust-chamber wall contours. These design "fixes" generally require prolonged and costly cut-and-try experimentation; and, while they should receive considerable attention in our future thrust-chamber research, what is needed above all is a precise theoretical model of the entire combustion process that will account for the combustion-oscillation characteristics as well as the combustion-efficiency characteristics. Research of the type described in the preceding paper is directed toward the achievement of such a model. The complexity and diversity of this problem are such that a great deal of imaginative research, both analytical and experimental, must be conducted in order to expedite its solution.

EXHAUST NOZZLE

The exhaust nozzle converts the thermal energy resulting from combustion into kinetic energy and, hence, into thrust by expanding the combustion gases to high velocity. In the atmosphere the degree of conversion is limited, since a conventional rocket nozzle cannot expand gas to velocities corresponding to pressures below ambient without incurring an overall thrust loss. In space there is no fundamental limit to expansion, since the ambient pressure is essentially zero.

The effect of altitude, or ambient pressure, on nozzle performance is illustrated in figure 40–7. Specific impulse in pounds thrust per pound flow per second as a function of altitude is shown for two nozzles, one with an expansion area ratio of 13, the other with an expansion area ratio of 50. The propellant combination is liquid oxygen–kerosene. At low altitudes, the large nozzle overexpands the working fluid to the extent that considerable thrust and, hence, specific impulse is lost. In practice, the loss is less than shown on this curve. At some point the flow no longer remains attached to the wall of the nozzle, flow separation occurs and the thrust loss due to a negative pressure differential is reduced. At higher altitudes, the more complete expansion possible with the larger nozzle yields considerably higher performance. Thus, there are two entirely different problems in the design of this component. One is concerned with the rocket engine operating in an Earth-launch trajectory. Since the engine will traverse a broad range of ambient pressures,

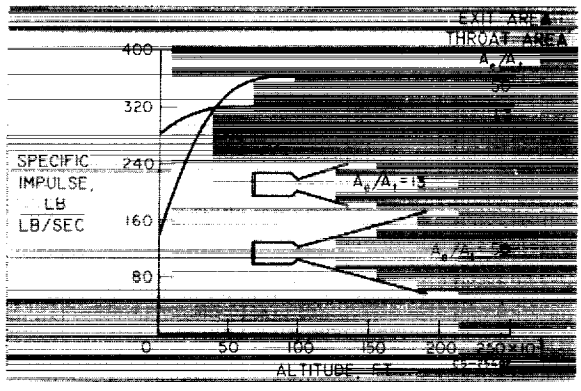

FIGURE 40–7.—Effect of altitude on nozzle performance.

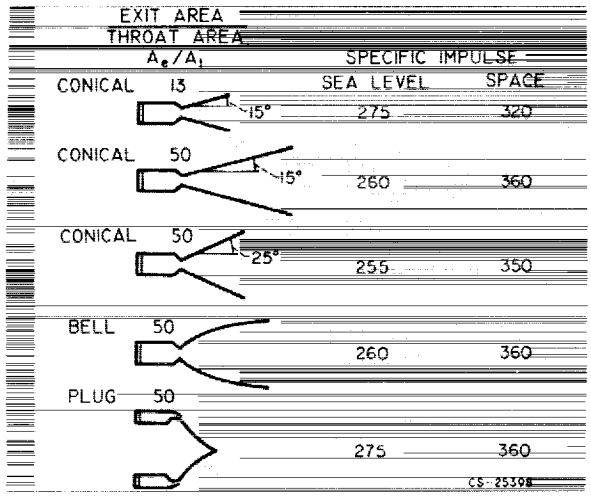

FIGURE 40–8.—Nozzle configurations and performance.

it cannot be designed to provide ideal expansion throughout its flight. A compromise design must be chosen to maximize the integrated impulse over the intended trajectory. The problem prompts investigation of potentially more flexible nozzle designs that may allow near-optimum expansion over a wider pressure range. For propulsion in space, the nozzle is designed to achieve the highest degree of expansion possible within the size envelope allowable in the vehicle and without imposing overall weight penalties on the vehicle.

Some design approaches that have been taken in the development of high performance, lightweight rocket nozzles are illustrated in figure 40–8. The first and second designs represent the low- and high-area-ratio nozzles of the preceding figure. These are 15° conics with sea-level and space specific-impulse values as noted. One approach to decreasing the size and the weight of the large-area-ratio space nozzle is to increase the divergence angle, as represented by the third design. Because of the increased divergence, there is a larger nonaxial component of thrust produced by the existing gas; hence, some performance is lost. The fourth design is the contoured or "bell" nozzle. The contouring allows expansion performance at a given area-ratio equivalent to the 15° conical nozzle, but at only 75 to 80 percent of the length. Exit divergence loss is minimized in this design.

The last design is the "plug" nozzle, which essentially allows free expansion of the gases. It not only provides a very short length, but also it has the added advantage of selfadjustment of the exhaust flow to the ambient pressure conditions. Its performance tends to match that of a high-area-ratio nozzle at high altitude and that of a low-area-ratio nozzle at low altitudes. Thus, it represents an approach to the ideal booster nozzle. Some promising experimental work has been accomplished with this design; the disadvantages are found primarily in physical hardware problems. Severe wall-cooling problems result from the fact that the maximum heat-transfer rate, which occurs in the throat region, is also in the region of maximum surface area. Large amounts of cooling, or superior cooling techniques, would be required to assure adequate durability of this design.

In addition to the plug nozzle, a number of other promising designs have been proposed to improve off-design performance, weight, and size. These designs include shrouded, annular, reverse-flow, and expansion-deflection nozzles. Further theoretical analyses may evolve still others. High-thrust booster engines and high-area-ratio space engines alike have ever increasing needs for more compact, lighter weight nozzles.

One final factor affecting nozzle performance is the extent of chemical recombination. Experience has shown that all nozzles suffer, in varying degrees, losses in performance that result from the less than maximum recombination of the highly dissociated combustion gases. The actual loss is a function of the propellants used, the combustion conditions, and the nozzle-design factors. The problem is not yet amenable to design approaches. Present technology has not provided us with adequate means of measuring or characterizing the chemical kinetic processes occurring during expansion so that possible solutions may be evolved. The need for basic research on chemical recombination, particularly under low-pressure conditions, is clear.

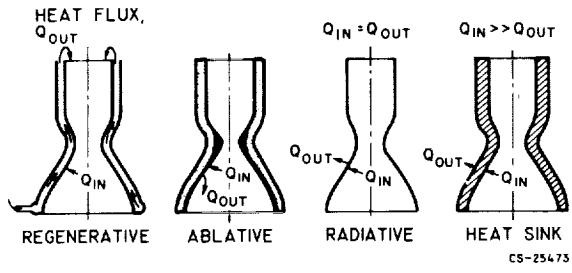

FIGURE 40–9.—Thrust-chamber cooling techniques.

DURABILITY

The last principal thrust-chamber requirement, durability, is closely related to nozzle design, combustion efficiency, and combustion stability. Large nozzles, and in particular some unconventional designs, impose increased cooling demands. Injectors that promote rapid combustion for high efficiency create injector and wall-cooling problems. Combustion instabilities can result in destructive levels of wall heat flux.

The four primary methods of cooling the walls of a thrust chamber are illustrated in figure 40–9. The first method is regenerative cooling, whereby one of the propellants, generally the fuel, flows through coolant passages in the wall of the thrust chamber prior to being injected into the combustion chamber. The second cooling method is ablation. The ablation process is basically one of dissipation of heat from the boundary layer by the decomposition and/or melting and vaporizing of the wall materials. While the regenerative chamber achieves equilibrium during operation, the ablative chamber continues to be eaten away and, hence, is a duration-limited system.

Most rocket thrust chambers that are in use today or are under development utilize one of these first two cooling methods. The third cooling method is radiation. The chamber wall in this case is a single thickness of high-temperature metal. Heat absorbed from the combustion process is radiated to space. The last method, the heat sink, has little application other than in research installations. The walls of a heat-sink chamber are made heavy enough to provide a sufficient heat capacity so that, for short duration operation, wall temperatures do not exceed the design limits.

Two additional basic methods of cooling are available to the thrust-chamber designer: (1) film cooling the wall by introducing a fraction

of the flow of one propellant near the wall, and (2) transpiration cooling by introducing a part or all of one propellant through a porous liner in the chamber. Both methods tend to incur serious performance penalties and, hence, have not been used to any extent as a primary cooling scheme. Film cooling in particular, however, is frequently applied to augment the primary cooling scheme.

Most of the current research on regeneratively cooled chambers has been directed toward the application of hydrogen for cooling of hydrogen-oxygen thrust chambers. This fuel is an excellent coolant because of its high heat capacity and because it does not decompose as do some fuels, for example, hydrazine. Because of these excellent cooling capabilities, hydrogen-oxygen thrust chambers that are now under development could be designed rather conservatively. The coolant is, in general, more than adequate for the job. Two areas of future activity, however, will involve greatly increased heat-flux conditions; the cooling margin will diminish, and more precise predictions of the heat-transfer characteristics will be required. In particular, local rather than overall heat transfer and transient as well as steady-state conditions will need consideration. One of these areas is the hydrogen-fueled, nuclear heat-transfer rocket; the other is the compact, high-pressure, high-thrust chemical rocket. Figure 40–10 is a plot of the relative value of heat-transfer coefficient for hydrogen against the ratio of wall to bulk-coolant temperature. The different curves represent correlations by different experimenters. The solid portions of the curves represent the ranges of experimental data; the dash portions represent the extrapolations. For temperature ratios currently encountered, the correlations represented predict about the same value of heat-transfer coefficient. The nuclear rocket and the high-pressure chemical rocket, however, will involve coolant-side heat transfer at wall-to-bulk-coolant temperature ratios that are well beyond the experimental conditions. The cooling potential of hydrogen at these very high heat-transfer rates must be precisely determined. Tube-type heat-transfer experiments under boiling and nucleate boiling conditions are needed. Also, the cooling requirements of these high heat-flux applications are not yet sufficiently well understood. The achievement of precise methods of predicting local as well as overall heat-flux rates will require analytical studies coupled with high heat-flux thrust-chamber tests.

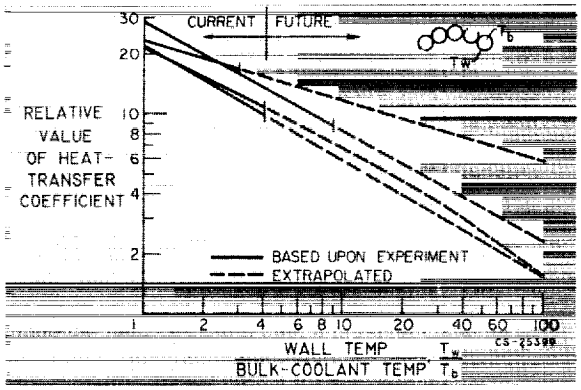

FIGURE 40–10.—Heat-transfer correlations over a range of wall-to-bulk-coolant temperature ratios.

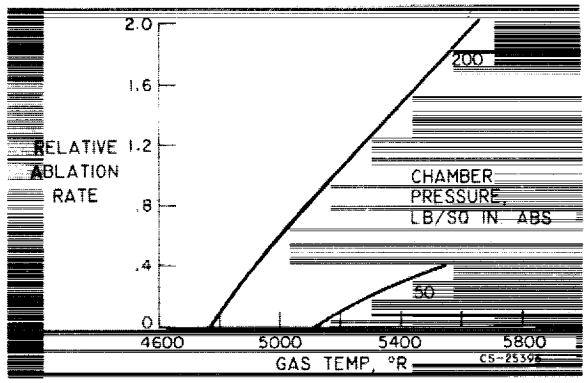

FIGURE 40–11.—Thrust-chamber ablation rates.

The durability of an ablatively cooled thrust chamber is represented by its ablation rate, the rate at which material is removed from the wall. The variation of ablation rate with gas temperature and combustion pressure is illustrated in figure 40–11. It can be seen that ablation rate increases rapidly as temperature is increased and that higher pressures also result in higher ablation rates. These data imply that the application of ablation cooling may be restricted to relatively low-pressure systems. While such systems are feasible for low-thrust application, they become impractical for high thrust appli-

cations. For example, the design of a 50-pounds-per-square-inch booster engine of 1,500,000-pounds thrust would require a combustion chamber with a diameter of about 14 feet. The temperature effect on ablation cannot be easily circumvented by design since high performance generally means high gas temperatures.

Much of the ablative material technology that is in use today for rocket engines has stemmed from atmospheric reentry hardware developments. The conditions are so different that optimum materials for the reentry condition are not necessarily also optimum for the rocket chamber walls. Therefore, considerably more effort needs to be expended on materials research specifically for rocket thrust chambers in an effort to develop ablative materials that are better able to withstand higher gas temperatures and higher pressures.

Radiation cooling is also restricted to special applications that involve low heat flux conditions, for example, nozzle extensions and very-low-pressure combustion systems. Surface temperatures of a radiation-cooled chamber are above the melting points of many of the more conventional alloys. The kinds of materials that must be considered include molybdenum, tungsten, and tantalum; fabrication techniques for these materials must be advanced if they are to be applied to thrust chambers. Even at wall temperatures well below the melting point of the material, durability can be considerably reduced by rapid corrosion of the walls. This problem calls for research on high-temperature protective coatings. Such coatings must withstand thermal shocks and vibrations.

SUMMARY

This brief review of the state of the art of the chemical-rocket thrust chamber has considered its principal requirements: ignition, combustion, exhaust-nozzle expansion, and durability. In each of these areas, the hardware technology required to produce satisfactory systems for today's needs is generally available. Additional research and development, however, is required to provide a better understanding of the processes involved so that new requirements can be met without repeating a multitude of cut-and-try experiments. Many areas exist where improved performance and increased operational flexibility would be highly desirable and, in fact, will be necessary for sophisticated space missions.

The kinds of problems that have been discussed relate to a number of basic fields of study. Analytical and experimental research is needed on ignition processes, including catalysis; the physics of propellant atomization and mixing; combustion dynamics; fluid flow and heat transfer under high-heat-flux conditions, nozzle aerodynamics, and high-temperature materials with particular emphasis on ablative compositions. This research is most urgently needed for the development of hydrogen-oxygen rocket systems but should also recognize potential future applications of other high-energy propellant combinations such as hydrogen-fluorine.

BIBLIOGRAPHY

The following is a bibliography of selected references pertaining to the liquid-propellant rocket thrust chamber.

AUBLE, CARMON M.: A Study of Injection Processes for Liquid Oxygen and Gaseous Hydrogen in a 200-Pound-Thrust Rocket Engine. NACA RM E56125a, 1956.

BLOOMER, HARRY E., ANTL, ROBERT J., and RENAS, PAUL E.: Experimental Study of Effects of Geometric Variables on Performance of Contoured Rocket-Engine Exhaust Nozzles. NASA TN D-1181, 1962.

CAMPBELL, C. E., and FARLEY, J. M.: Performance of Several Conical Convergent-Divergent Rocket-Type Exhaust Nozzles. NASA TN D-467, 1960.

CONNORS, JAMES F., CUBBISON, ROBERT W., and MITCHELL, GLENN A.: Annular Internal-External-Expansion Rocket Nozzles for Large Booster Applications. NASA TN D-1049, 1961.

CURREN, ARTHUR N., PRICE, HAROLD G., JR., and DOUGLASS, HOWARD W.: Analysis of Effects of Rocket-Engine Design Parameters on Regenerative-Cooling Capabilities of Several Propellants. NASA TN D-66, 1959.

FARLEY, JOHN M., and CAMPBELL, CARL E.: Performance of Several Method-of-Characteristics Exhaust Nozzles. NASA TN D–293, 1960.

FEILER, CHARLES E., and YEAGER, ERNEST B.: Effect of Large-Amplitude Oscillations on Heat Transfer. NASA TR R–142, 1962.

GORDON, SANFORD, and MCBRIDE, BONNIE J.: Theoretical Performance of Liquid Hydrogen with Liquid Oxygen as a Rocket Propellant. NASA MEMO 5–21–59E, 1959.

GREGORY, JOHN W., and STRAIGHT, DAVID M.: Ignition of Hydrogen-Oxygen Rocket Combustor with Chlorine Trifluoride and Triethylaluminum. NASA TN D–684, 1961.

HEIDMANN, M. F., and BAKER, LOUIS, JR.: Combustor Performance with Various Hydrogen-Oxygen Injection Methods in a 200-Pound-Thrust Engine. NACA RM E58E21, 1958.

HENDRICKS, R. C., GRAHAM, R. W., HSU, Y. Y., and FRIEDMAN, R.: Experimental Heat Transfer and Pressure Drop of Liquid Hydrogen Flowing Through a Heated Tube. NASA TN D–765, 1961.

LADANYI, DESZO, J. and MILLER, RILEY O.: Comparison of Ignition Delays of Several Propellant Combinations Obtained with Modified Open-Cup and Small-Scale Rocket Engine Apparatus. NACA RM E53D03, 1953.

LOVELL, J. CALVIN, SAMANICH, NICK E., and BARNETT, DONALD O.: Experimental Performance of Area Ratio 200, 25 and 8 Nozzles on JP–4 Fuel and Liquid-Oxygen Rocket Engine. NASA TM X–382, 1960.

MALE, THEODORE, KERSLAKE, WILLIAM R., and TISCHLER, ADELBERT O.: Photographic Study of Rotary Screaming and Other Oscillations in a Rocket Engine. NACA RM E54A29, 1954.

NEU, RICHARD F.: Injection Principles for Liquid Oxygen and Heptane Using Nine-Element Injectors in an 1800-Pound-Thrust Rocket Engine. NACA RM E57E13, 1957.

PRIEM, RICHARD J., and HEIDMANN, MARCUS F.: Propellant Vaporization as a Design Criterion for Rocket-Engine Combustion Chambers. NASA TR R–67, 1960.

RAO, G. V. R.: Recent Developments in Rocket Nozzle Configurations. ARS Jour., vol. 31, no. 11, Nov. 1961, p. 1488.

RIEHL, W. A., PERKINS, HAROLD, STOKER, CHARLES S., and KIRSHENBAUM, A. D.: Ozone Fluoride for Rocket Propulsion, ARS Jour., vol. 32, no. 3, Mar. 1962, p. 384.

ROBBINS, WILLIAM H.: Analysis of the Transient Radiation Heat Transfer of an Uncooled Rocket Engine Operating Outside Earth's Atmosphere. NASA TN D–62, 1959.

ROLLBUHLER, R. JAMES, and STRAIGHT, DAVID M.: Ignition of a Hydrogen-Oxygen Rocket Engine by Addition of Fluorine to the Oxidant. NASA TN D–1309, 1962.

RUPE, JACK H.: A Correlation Between the Dynamic Properties of a Pair of Impinging Streams and the Uniformity of Mixture-Ratio Distribution in the Resulting Spray. Progress Rep. 20–209, Jet Propulsion Laboratory, Pasadena, Calif., Mar. 1956.

SIEVERS, GILBERT K., TOMAZIC, WILLIAM A., and KINNEY, GEORGE R.: Theoretical Performance of Hydrogen-Oxygen Rocket Thrust Chambers. NASA TR R–111, 1961.

SUTTON, GEORGE P.: Rocket Propulsion Elements. Second ed., John Wiley & Sons, Inc., 1956.

41. Dynamics and Control of Chemical Rockets

By John C. Sanders and Leon M. Wenzel

JOHN C. SANDERS *is Technical Consultant for Development in the Advanced Development and Evaluation Division of the NASA Lewis Research Center. Currently concerned with nuclear rocket research, he has specialized in aircraft and spacecraft powerplants and propulsion systems with particular emphasis on application of controls to these systems. He attended Virginia Polytechnic Institute, receiving B.S. and M.S. degrees in Mechnical Engineering in 1936 and 1937, respectively. He is a member of the American Society of Mechanical Engineers and the Institute of the Aerospace Sciences.*

LEON M. WENZEL, *Aerospace Scientist at the NASA Lewis Research Center, is currently working on the application of large hydrogen-oxygen rocket engine systems and on systems analysis. He graduated from Ohio Northern University with a B.S. degree in Electrical Engineering in 1954.*

INTRODUCTION

Some of the problems will be examined herein that arise when a complete propulsion system is assembled. The problems discussed are dynamic ones—the problems of system stability and control. In the interest of brevity, the problems will be illustrated by reference chiefly to the hydrogen-oxygen rocket. After describing some possible rocket systems and some of the necessary control functions, the study will delve into dynamic properties of components of rocket systems that influence system stability and control. Then some of the effects of component dynamics on system stability, design, operation, and control will be illustrated.

DESCRIPTION OF COMPLETE ROCKET SYSTEMS

One of the rocket systems where pumps are used to supply propellants to the combustion chamber is shown in figure 41–1. The heat picked up by the hydrogen as it circulates through the coolant jacket of the combustion chamber and nozzle is sufficient to drive a turbine. The gas exhausted by the turbine is then injected into the combustion chamber. This pumping arrangement is called the topping cycle. Control in the topping cycle is achieved by manipulation of the turbine valve to regulate thrust and the mixture valve in the oxygen propellant line to maintain desired mixture ratio.

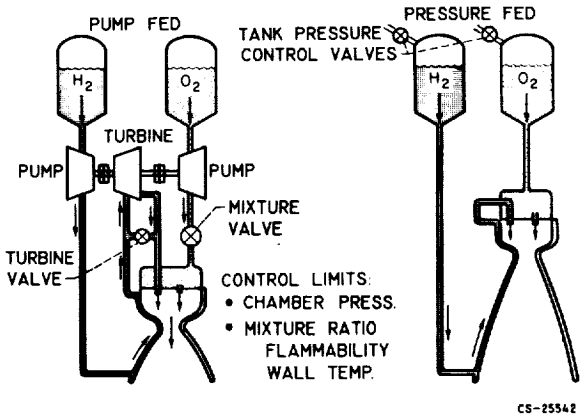

FIGURE 41–1.—Two flow systems for a chemical rocket.

A pressure fed engine is also shown in figure 41–1. The pressure in the propellant tanks is sufficient to force the two propellants through the injector into the combustion chamber. The hydrogen is first circulated through the coolant

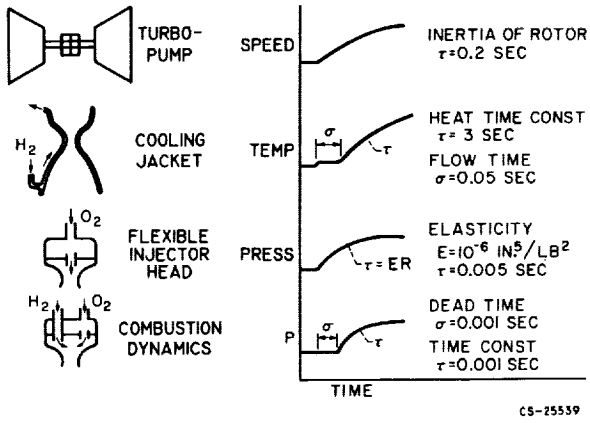

FIGURE 41-2.—Dynamics of components of a rocket system.

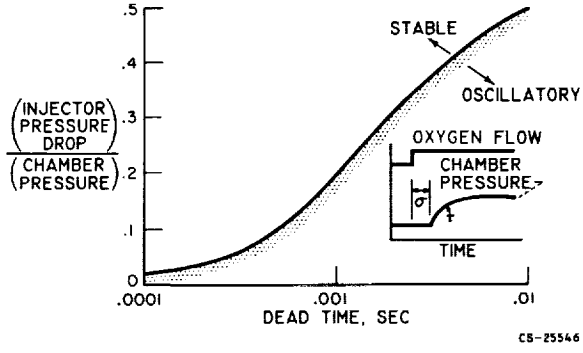

FIGURE 41-3.—Destabilizing effect of dead time on propellant flow system. Time constant, 0.001 second.

jacket. In the pressure-fed engine the pressures in the supply tank can be regulated to yield the desired chamber pressure and mixture ratio.

Among the control limits are chamber pressure (which is proportional to thrust), mixture ratio, and turbopump speed. High chamber pressure and high turbopump speed can cause injuriously high material stresses, and even rupture. Limits on mixture ratio are flammability limits and high gas temperature near stoichiometric mixture, which can cause overheating of the walls of the combustion chamber.

DYNAMICAL ELEMENTS OF ROCKET

Four of the elements of the rocket that contribute significantly to system dynamics are shown in figure 41-2. First is the turbopump. Its inertia causes a comparatively slow response of pump speed to a disturbance. The cooling jacket introduces the characteristic dynamics of a heat exchanger, which may be simplified to a rough approximation containing a heat-transfer term and a flow term. The elasticity of the injector is significant to high frequency stability, as are the combustion dynamics, herein described in terms of dead time and time constant.

COMBUSTION DYNAMICS

The properties of combustion dynamics and their significance in determining flow system stability are illustrated in figure 41-3. The figure shows that, if a step change in oxygen flow is introduced, the chamber pressure shows no change for a period σ, called the dead time. Then the pressure rises with a characteristic time constant τ. The dead time, which is associated with the drop atomization, mixing, and ignition, is more disastrous and less understood than the time constant, which is like an aerodynamic filling time.

The effect of this dead time on stability is shown in figure 41-3. In general, as the dead time increases, the injector pressure drop required to ensure stable propellant flow increases, thereby increasing the required supply pressure.

Operating conditions that influence dead time are shown in figure 41-4. The dead time is shown to decrease with increasing chamber pressure and decreasing oxidant-fuel ratio. It is possible that the injection velocity of the liquid propellant (oxygen, since the hydrogen is heated in the cooling jacket) is more significant than chamber pressure.

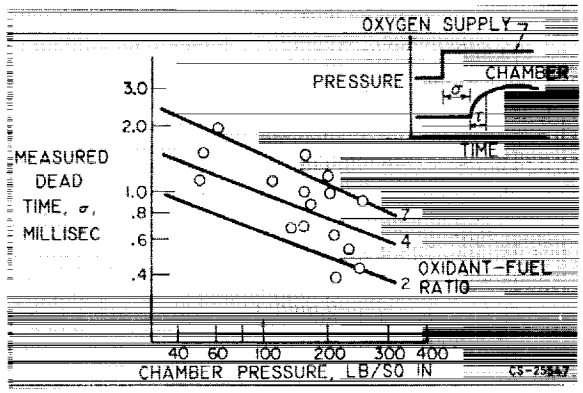

FIGURE 41-4.—Control dynamics of a rocket combustion chamber using hydrogen-oxygen propellant.

It is worthy to note the extremely short dead time for the hydrogen-oxygen propellant combination. Kerosene and other nonhypergolic storable propellants have dead times five times as great. With hydrogen-fluorine, on the other hand, the dead time has been immeasurably small. Thus, the order of stability from stable to unstable is: hydrogen-fluorine, hydrogen-oxygen, storable nonhypergolic.

STABILITY OF PRESSURE-FED ENGINE

One of the instances where instability plagues the propellant system is while "throttling" or reducing the thrust of a pressure-fed engine. This propensity to oscillate is the result of the low injector pressure drop encountered at low thrust. The injector pressure drop had been set at a low value even at full thrust to avoid tank pressure and high tank weight.

The stability bounds, shown as a function of throttle range for a selected rocket, are presented in figure 41–5. The throttle range is the ratio of maximum thrust to minimum thrust. In each curve, operation at oxygen pressure drop below the curve will result in oscillation at the minimum thrust.

An interesting feature of the figure is that reducing hydrogen injector pressure drop can be achieved by a moderate increase in oxygen pressure. Such a trade is desirable since the hydrogen tank is larger, and weight savings are realized at the lower tank pressure. The

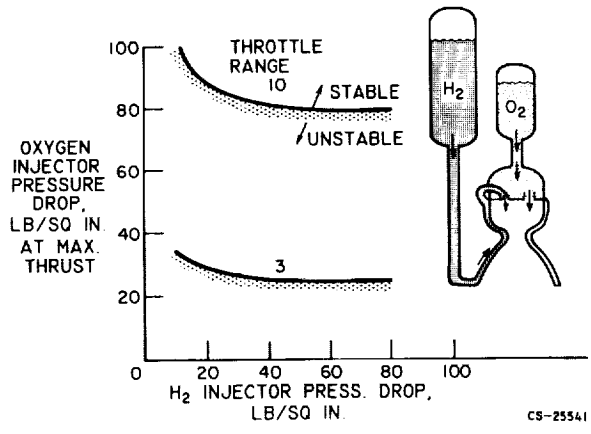

FIGURE 41–5.—Injector flow stability limits of hydrogen-oxygen engine. Dead time, 0.001 second; time constant, 0.00085 second; elasticity, 10^{-6} inch^5 per pound^2.

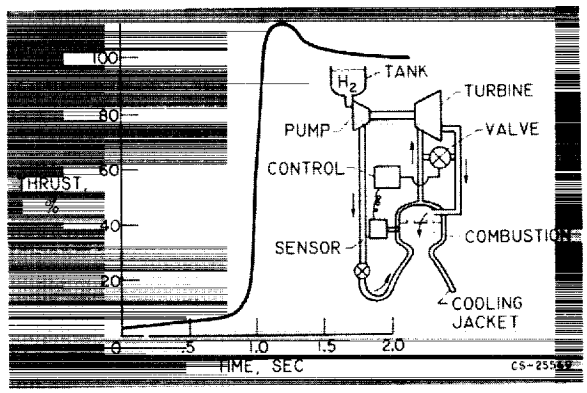

FIGURE 41–6.—Startup of a hydrogen-oxygen rocket-topping cycle (oxygen not shown).

reason for the insensitivity of stability limits to hydrogen injection pressure drop is the heating of the hydrogen in the coolant passages before injection. Also shown is the fact that high oxygen pressure drop must accompany large throttle ratio if stability is to be achieved. Throttle ratios as high as 10 have been obtained in tests.

STARTUP OF PUMP-FED ENGINE

The startup transient of the pump-fed engine is influenced by pump inertia, turbine torque, and particle passage time through the coolant jacket more than by combustion-chamber dynamics. An idea of the quickness of acceleration may be obtained from Figure 41–6. The rapidity with which the thrust approaches maximum shows that an accurate, quick-acting control is needed to prevent going to such high overload that damage is incurred. Control frequency responses up to 10 cycles per second are needed.

THRUST MANIPULATION WITH PUMP-FED ROCKET

Once the rocket has been started, the problems arise of manipulating the thrust to desired values quickly and stably. In the problem of injector system instability previously discussed, additional problems associated with the pump are encountered. Two of these pump problems are pump stall and flow instability resulting from a static characteristic of the pump.

These problems are illustrated in Figure 41–7, where deceleration from full thrust at point

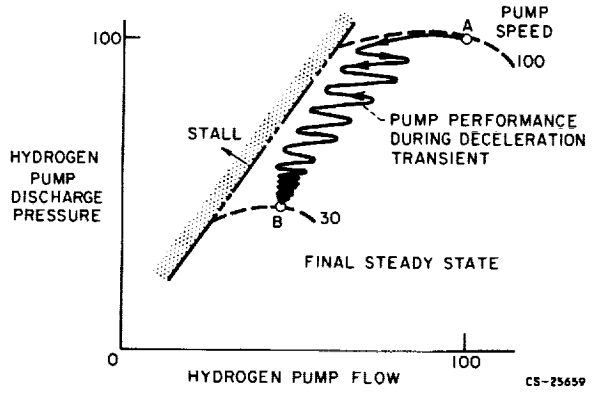

FIGURE 41–7.—Oscillations in a rocket flow system induced by pump flow characteristics.

A to a lower thrust at point B was attempted. A rather severe oscillation was induced, and the stall limit was approached with a dangerously small margin. The cause of the oscillation was traced to the slope of the pump pressure delivery characteristic at constant speed. A positive slope produces a less stable flow system than does a negative one. Inspection of Figure 41–7 shows that the deceleration transient caused the pump to operate in a less stable positive slope region. Furthermore, at the lower thrust level, point B, the steady-state operating point is in a less stable operating region (more positive slope of pump characteristic) than point A. Throttling to an even lower operating point than B could have resulted in failure of the system to even reach steady state. The results shown were obtained from an analog computer study that simulated an actual experience.

Thus, the figure shows that oscillation of the entire flow system can be induced by a positive slope of the pump characteristic and that the steady-state throttling range can also be limited by the same pump characteristic.

FURTHER WORK NEED ON CHEMICAL ROCKETS

The technology of control and dynamics of chemical rockets is far advanced as a result of long intensive research and development. Dynamics of combustion, however, are worthy of further investigation, although many investigators have worked in this field. Only in the very simple chemicals has the knowledge of dynamics reached a degree of usefulness, and even here the dynamics at low pressure are not thoroughly developed. Certain knowledge of the dynamics of storable propellants useful for course corrections and of attitude control of a space vehicle would improve the capability to modulate the thrust, and thereby enhance the usefulness of these propellants.

BIBLIOGRAPHY

DRAIN, DANIEL I., SCHUM, HAROLD J., and WASSERBAUER, CHARLES A.: Relations of Combustion Dead Time to Engine Variables for a 20,000-Pound-Thrust Gaseous-Hydrogen–Liquid-Oxygen Rocket Engine. NASA TN D–851, June 1961.

HURRELL, HERBERT G.: Analysis of Injection-Velocity Effects on Rocket Motor Dynamics and Stability. NASA TR R–43, 1959.

OTTO, EDWARD W., and FLAGE, RICHARD A.: Experimental Studies of Combustion Chamber and Feed System Stability During Throttling of a Regeneratively Cooled Liquid Hydrogen-Fluorine Rocket Engine. Paper 246B, SAE, Oct. 10–14, 1960.

Concluding Remarks

By Walter T. Olson

For a somewhat detailed picture of certain key technology in the chemical-rocket field, it is necessary to discuss one thing at a time. In real life, however, things usually do not happen one at a time. Thus, the importance of viewing a propulsion system as a system must be stressed.

In order to achieve needed reliability in future high-performance systems of increasing sophistication, high quality must be specified and designed into all components at inception. Problems arising from unfavorable interactions of components also must be avoided. The paper by John C. Sanders and Leon M. Wenzel has detailed some examples in system dynamics; some further examples selected from past occurrences and experiences are: (1) The pump blades should not stimulate or excite resonant frequencies in such tender parts as an injector face. (2) The state and the flow rate of gas to drive a turbopump must be controlled to keep the pump flows within the stall and the surge limits of the pumps; and, to complicate matters, the pump delivery, in turn, may be affecting the gas flow to the turbine. (3) The cooling passages of a thrust chamber must accommodate the local heat transfer, which, in turn, is strongly a function of the combustion pattern produced by the injector design. (4) Propellant-flow lines can be harmfully in tune or safely out of tune with fluctuating gas pressure in the combustor. (5) Pump design must allow for enough delivery pressure to ensure enough pressure drop for cooling needs and for injection with stable combustion.

Reliability is a quality in the initial concept of the complete system and its parts. The designs and systems that are being and will be created are too intricate and specialized, and the performance of their components is too interrelated for uninformed tinkering. A development must start right, not just because subsequent attempts at fixes may be costly and time consuming, but also because fixes may be impossible.

There is a continuing need for emphasizing training in the basic principles of engineering and science, so that even while working on a specialty the engineer or scientist will have a broad, interdisciplinary point of view. The scientists and engineers that are trained for the future must have the ability to see the problems of whatever they undertake with clarity and completeness. Such comprehension comes by use of the fundamental principles of physics, chemistry, mechanics, metallurgy, electricity, etc., to create a conceptual quantitative model of the device or the system. Both high-quality components and their harmonious blending come from an understanding and appreciation of the physical processes and phenomena at work in a particular operation.